Effect of trough and dipping parameters on Langmuir and Langmuir-Blodgett thin films of PVDF using MEK solvent

A thesis

Submitted in the partial fulfillment of the requirement for the award of degree of

MASTER OF SCIENCE

in

PHYSICS

Submitted by

Isha Kalra

(Roll No. 301604015)

Under the guidance of

Dr. Loveleen Kaur Brar

Assistant Professor

School of Physics and Materials Science

Thapar Institute of Engineering and Technology, Patiala-147004

June-2018

Dedicated to

My family and friends

for their love and support

CERTIFICATION

I hereby certify that this thesis entitled, "***Effect of trough and dipping parameters on Langmuir and Langmuir-Blodgett thin films of PVDF using MEK solvent***" in fulfillment for the requirements for the award of Degree of Master of Science in Physics submitted to School of Physics and Material Science, Thapar Institute of Engineering and Technology, Patiala, is an authentic record of my own work and is carried under the supervision of **Dr. Loveleen Kaur Brar**. The matter submitted via this thesis report has not been submitted for the award of any other degree to the best of our knowledge.

Date: 04/08/18 **Isha**

Place: TIET, Patiala **(301604015)**

This is to certify that the above statement made by the candidate is correct and true to the best of my knowledge.

Dr. Loveleen Kaur Brar
Assistant Professor
TIET, Patiala- 147004

ACKNOWLEDGEMENT

Several people have collaborated in the accomplishment of my M.Sc. thesis.

It is a genuine pleasure to express my deep sense of gratitude and appreciation to my M.Sc. dissertation thesis supervisor and philosopher, **Dr. Loveleen Kaur Brar** Assistant Professor, SPMS, Thapar Institute of Engineering and Technology, Patiala for her dedication, inspiration and keen interest. Her overwhelming attitude has been solely responsible for the completion of my work.

I wish to express my sincere thanks to **Dr. Manoj Kumar Sharma**, Head and Professor, SPMS, Thapar Institute of Engineering and Technology, Patiala-147004 for his support and guidance.

I would be remiss if i do not thank **Dr. Puneet Sharma** and **Dr. B.N. Chudasama**, SPMS, Thapar Institute of Engineering and Technology, Patiala for their valuable help.

A special word of thanks to **Ms. Raveena Chaudhary** for her valuable guidance and suggestions. I approached her any time and she was there to help me.

I am also thankful to my fellow mates, **Ms. Kaveri Ajravat** and **Mr. Ajit Seth** for helping me in the experiments. I acknowledge their co-operation.

Finally, I would like to express my gratitude and love to my family for their wise counsel and sympathetic ear. They have always believed in me and supported me. In addition I would like to thank **Mr. Anshul Kashyap** for helping me to keep things in perspective.

04/08/18

Date: ~~June~~ Aug, 2018

Isha

Abstract

Poly vinylidene fluoride (PVDF) in the form of thin films finds multiple applications such as actuators for sound reduction, pressure sensors, piezo-actuators and reusable PVDF sensors to detect the structural faults due to high thermal stability, ultra sensitivity, high deformability and chemical resistance. The β-phase of PVDF homoploymer is the most promising phase of this material which can meet the hot spot for applications in piezoelectricity, pyroelectricity and ferroelectricity. Langmuir-Blodgett (LB) technique is useful for the formation of a highly organized assembly of amphiphilic molecules which can be transferred onto a solid substrate. The work presented in this thesis is aimed at synthesizing homopolymer PVDF LB films to expand their applications. PVDF swells up when dissolved in Methyl ethyl ketone (MEK) which is taken as the spreading solvent in the present work. To obtain good transfer characteristics the PVDF monolayers on the water surface were characterized for different compression rates and subphase temperature. The isotherm, hysteresis and barrier oscillation experiments show that the most stable PVDF films were obtained at 20 ˚C for 10 mm/min compression rate. These trough parameters were used for the deposition of the LB films. An important result to emerge from these experiments was that even though the MMA of the solid phase does not change significantly with the temperature range under consideration dissolution of the deposited film, the enhanced kinetic energy drastically reduces the elasticity of the solid phase at higher temperatures. The dipping experiments show that very good TR can be obtained for the first upstroke for 2 mm/min substrate speed. But down stroke results in partial desorption and reduced TR in subsequent upstrokes. This indicates that PVDF LB films are Z-Type in nature. But the Z-Type nature gets disrupted due to the partial dissolution of PVDF into water during downstrokes. To avoid this the subphase was changed after every single layer deposition. Transparent films of PVDF were synthesized by deposition of 1, 4 and 8 layers on the hydrophilic substrate followed by drying and annealing. The topographic analysis of the final films shows the emergence of few large crystallites which makes the films rough.

CONTENTS

S. No.	Title	Page No.
	List of figures	**ix**
	List of tables	**xi**
Chapter 1	**Introduction to PVDF thin films**	
1.1	Thin films	1
1.2	Significance of thin films	1
1.3	Poly (vinylidene) Fluoride (PVDF)	2
1.4	Polymorphism in PVDF	3
1.5	β-phase PVDF- an ideal polymorph	4
1.6	PVDF thin films	5
1.7	Applications of PVDF thin films	6
1.8	References	6
Chapter 2	**Langmuir- Blodgett deposition technique**	
2.1	Langmuir monolayer	8
2.2	Langmuir- Blodgett monolayer	8
2.3	Gas- liquid interface	8
2.4	Surface tension	8
2.5	LB monolayer materials	9
2.6	Surface pressure- area isotherms	9
2.7	Effect of compression rate	10
2.8	Effect of subphase temperature	11
2.9	Hysteresis	11
2.10	Barrier Oscillation	12
2.11	Instrumental setup for LB technique	12
2.12	Film deposition mechanism	14
2.13	Deposition modes	15
2.14	Transfer ratio	15
2.15	References	16

Chapter 3 Literature review

3.1 Deposition of Langmuir- Blodgett thin films 17

3.2 Characterization of Langmuir monolayers using Langmuir troughs 18

3.3 Synthesis of PVDF thin films using various techniques 19

3.4 Synthesis of PVDF thin films using Langmuir-Blodgett technique 20

3.5 References 21

Chapter 4 Materials and methods

4.1 Materials 22

4.2 Methods 23

4.2.1 Cleaning of barriers and trough 23

4.2.2 Preparation of precursor PVDF solution 23

4.2.3 Preparation of subphase (de-ionized water) 24

4.2.4 Substrate cleaning 24

4.2.5 Spreading of Langmuir monolayer 24

4.3 Deposition of LB monolayer on the substrate 24

4.3.1 Drying and calcination conduct 24

4.4 Characterization techniques 24

4.4.1 Surface pressure- area isotherms 24

4.4.2 Hysteresis 25

4.4.3 Barrier Oscillations 25

4.4.4 Atomic force Microscopy (AfM) 25

4.5 References 26

Chapter 5 Results and discussion

5.1 Surface pressure- area isotherms 27

5.1.1 Effect of compression rate 27

5.1.2 Effect of subphase temperature 28

5.1.3 Hysteresis 30

5.2 Oscillating barrier characterization of PVDF thin films 32

5.2.1 Effect of barrier oscillation frequency 32

5.2.2 Oscillation of barriers at different compression rates 35
5.2.3 Oscillation of barriers at different subphase temperature 37
5.3 Deposition of PVDF Langmuir- Blodgett films 40
5.4 Atomic Force Microscopy (AFM) 40
5.5 References 42
Chapter 6 Conclusion and Future scope
6.1 Conclusion 43
6.2 Future scope of work 43

List of Figures

Figure No.	Description	Page No.
1.1	Various applications of thin films	2
1.2	(a)Schematic representation of Poly (vinylidene) fluoride repeating units (b)Structure of PVDF	2
1.3	Four crystalline polymorphs of PVDF with different alignment of –H and –F bonds	4
1.4	Schematic showing formation of β-phase from α-phase	5
1.5	a) Random orientation of dipoles in β-phase without electric field b) Aligned dipoles due to electric field	5
2.1	Amphiphilic molecule with distinguished hydrophobic and hydrophilic parts	9
2.2	Schematic of surface pressure- area isotherm	10
2.3	Schematic of Π-A isotherm at different compression rates	11
2.4	Hysteresis curve of surface pressure- area isotherm	12
2.5	Langmuir- Blodgett setup	13
2.6	Wilhelmy plate partially immersed in subphase surface	13
2.7	Deposition of film on a substrate	14
2.8	Different modes of Langmuir- Blodgett film deposition	15
4.1	Schematic of orientation of PVDF molecules on the surface of water**:** O-H groups forms hydrogen bonds with the C-F molecules of PVDF	22
4.2	Structure of MEK	23
4.3	(a) Schematic diagram of AFM depicting general components (b) Laboratory view of AFM used	25
5.1	***Effect of compression rate*** a) Π- A isotherms for PVDF at 20˚C on DI water for spreading volume of 100 μL b)Variation of MMA of solid and liquid phase and static elasticity of solid phase with different compression rates	28
5.2	***Effect of subphase temperature*** a) Π-A isotherms for	29

	PVDF at 10 mm/min barrier speed for a spreading volume of 100μL b) Variation of MMA of solid and liquid phasesand static elasticity of solid phase with different subphase temperatures.	
5.3	a) Π-A hysteresis isotherms of PVDF monolayer for 5 cycles b) Compression isotherms hysteresis at rate 10 mm/min with spreading volume 100μL and subphase temperature 20˚C	30
5.4	Variation of MMA of liquid and solid phase and Static elasticity with the number of cycles.	31
5.5	Surface pressure variations with time at different oscillation frequencies for PVDF monolayer with barrier speed 10 mm/min	33
5.6	Variation of |G|, G', G" with different barrier oscillations frequencies.	34
5.7	*Π*- variations for barrier oscillation experiments at different compression rates	35
5.8	Variation of |G|, G' and G" at different compression rates for PVDF monolayer	36
5.9	Surface pressure variations for barrier oscillation experiments at different subphase temperatures with barrier speed 10 mm/min and frequency of oscillation as 25 mHz	37
5.10	Variation of G, G' and G" with subphase temperature	38
5.11	**(a-c)** Variation of Transfer ratio (TR) with No. of layers of PVDF monolayer at different dipping parameters with surface pressure target 30 mN/m.	39
5.12	AFM images of PVDF LB films on glass substrate **a)** 20 μm × 20 μm image of 1 layer **b)** 1 μm ×1 μm, image of 1 layer film in the smoother region **c)** 20 μm × 20 μm image of 4 layer film **d)** 15 μm × 15 μm image of 8 layer film.	41

List of Tables

Table No.	Descriptions	Page No.
1.1	Material properties of PVDF	3
5.1	Mean molecular area (MMA) of liquid and solid phase and static elasticity of solid phase for different compression rates	27
5.2	MMA of liquid and solid phase and static elasticity of solid phase for different subphase temperatures.	29
5.3	MMA and static elasticity of liquid and solid phases for successive compression cycles during hysteresis study.	31
5.4	Dynamic viscoelastic properties at different oscillation frequencies	34
5.5	Dynamic viscoelastic properties obtained from the analysis of the curves at different rates of compression.	36
5.6	Dynamic viscoelastic properties obtained from the analysis of curves at different subphase temperatures.	38
5.7	Roughness analysis of the AFM images	41

Chapter 1

Introduction to PVDF thin films

1.1 Thin films

A thin film is defined as a coating or layer of material whose thickness may vary from a few nanometers to several micrometers. The properties of any material are remarkably different when examined in the form of a thin film. Several studies on thin films have led to the advancement in many research areas of solid state physics and chemistry which are based on the distinctive characteristic of geometry, thickness and structure of the film [1].

The natural world also consists of various examples of thin film layers such as:

- Soap bubble formation
- Shiny feathers of birds
- Wings of butterflies (peacock butterfly) and insects [2]
- Oil slicks
- A gloss like appearance on the petals of certain flowers (Buttercup flowers)

The variation in the properties of thin films from the bulk is mostly due to the reduction in the size of the particles of the material, i.e. formation of nanostructures. This is known as quantum confinement effect.

1.2 Significance of thin films

Thin film technology is the fundamental cause of the impressive development in the diverse fields of optoelectronics, photonics, space and science, aircrafts, defense, etc. Both crystalline and amorphous thin films have an immense use in age of advancement. Many attractive properties are associated with thin films which are responsible for their versatility. Less space is occupied by the devices made from thin films. The understanding and formation of thin films onto a substrate encompasses various disciplines (Fig1.1) [1].

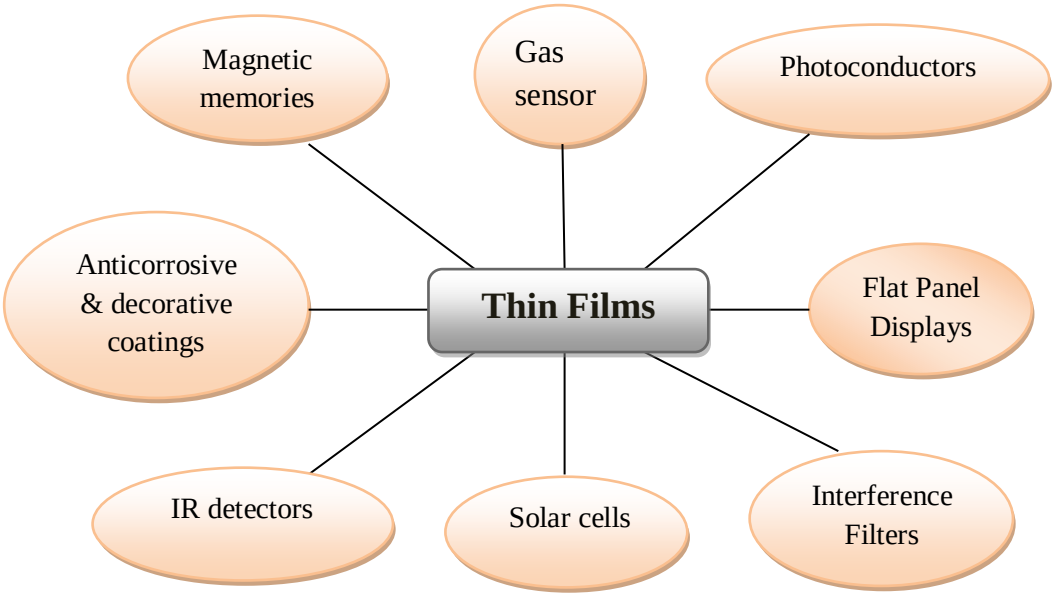

Fig. 1.1 Various applications of thin films.

1.3 Poly (vinylidene) fluoride (PVDF)

PVDF is a typical semi-crystalline thermoplastic polymer. It is a fluoropolymer and is about 50% amorphous mostly synthesized by the free radical polymerization of 1,1-difluoroethylene. The monomer has the structure -CH_2-CF_2- with 'head to tail' chain configurations. Some of its essential properties are listed below in the table 1.1.

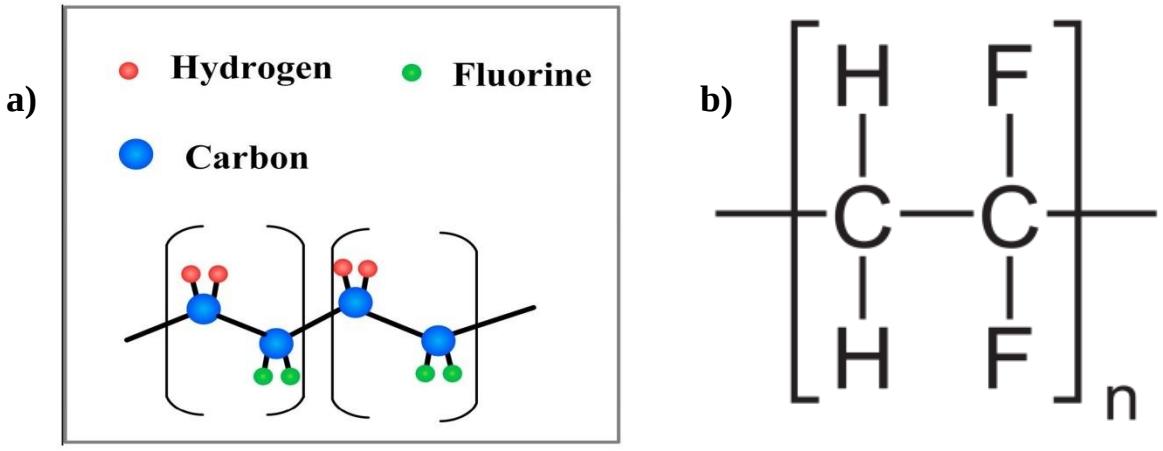

Fig. 1.2 a) Schematic representation of Poly (vinylidene) fluoride repeating units
b) Structure of PVDF [9].

Table1.1 Material Properties of PVDF [3]

Chemical Formula	$-(C_2H_2F_2)_n-$
Density	1.78 g/cm^3
Appearance	Whitish solid
Solubility in water	Insoluble
Melting Point	160-170˚C
Curie Temperature	103˚C
Glass transition temp (T_g)	-35˚C
Dielectric constant	7.7 (for 10Hz)

PVDF is a useful polymer due to its chemically resistant nature, stability towards various radiations like UV, Gamma & X-rays, non-toxicity, high dielectric strength and resistance towards heat, combustion & ageing. The polymer is unique due to its ferroelectric properties and the piezoelectric response which is much stronger when compared to other polymers.

1.4 Polymorphism in PVDF

In polymers, a rotation is possible along the C-C bond. This results in a wide range of conformations. Two staggered states can be identified in the PVDF polymer, namely Gauche (G) and Trans (T). Gauche states have high energy than the Trans. But when a polymer chain has the capability to crystallize, it has an extended conformation. This can be observed clearly because in a crystal, the need for regular arrangement favours highly ordered zig-zag shapes. Different conformations are adopted by the polymer chains to maximize their entropy.

There are four crystalline polymorphs of PVDF- α, β, γ and δ which can be converted to one another by temperature changes and external force.

α-phase $(TGT\bar{G})$ - This is the most common polymorph of PVDF. It is non- polar in nature due to the anti parallel arrangement of two connected chains. The unit cell is monoclinic.

β-phase (TT) - It is the most important polymorph because of a strong response towards piezoelectricity and high dielectric strength. It has more intermolecular stability due to the parallel arrangement of chains which makes it highly polar. The unit cell is orthorhombic.

γ-phase ($T_3GT_3\bar{G}$) -The γ- phase may or may not contain a parallel chain which subsequently leads to polar or non- polar nature. By applying some mechanical stress, it is converted into β-phase. The unit cell is orthorhombic.

δ- phase- It is the counterpart of the α-phase. The polar nature of δ- phase is due to the presence of the parallel chains. By the application of high electric field, α- phase is converted into δ-phase. It has the same unit cell as the α-phase [6, 7].

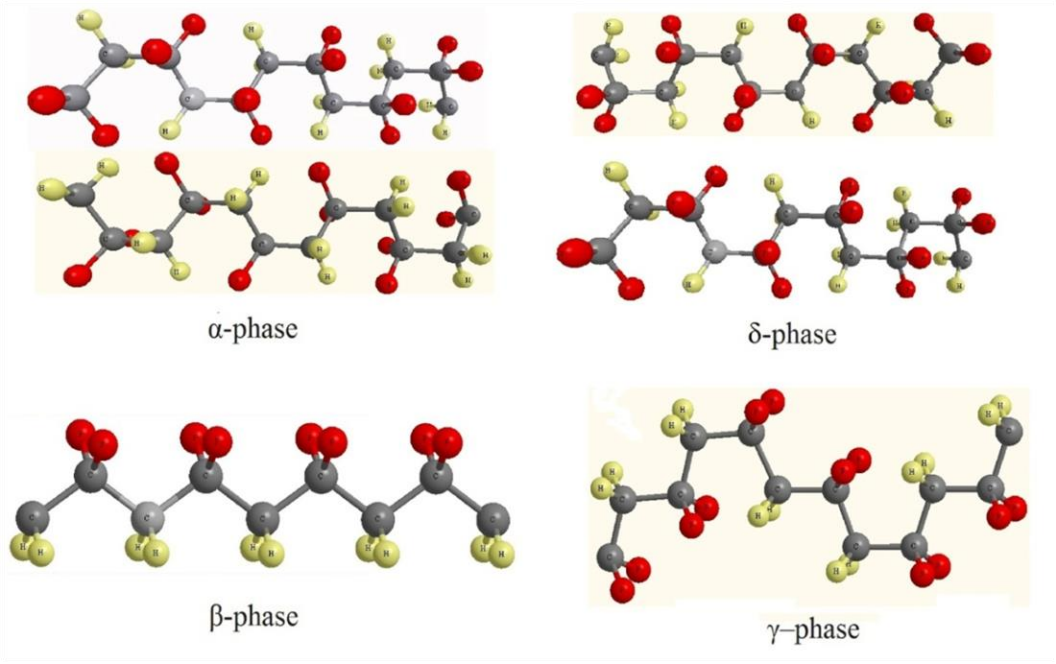

Fig 1.3 Four crystalline polymorphs of PVDF with different alignments of –H and –F bonds [6].

1.5 β- phase PVDF– an ideal polymorph

It is well known that PVDF is an 'ideal piezoelectric polymer'. Piezoelectric behaviour of all the PVDF crystalline forms depends on the alignment of dipoles. The arrangement of Hydrogen and Fluorine atoms in β- phase is highly polar due to which a net spontaneous polarization is present in the PVDF unit cell. After recrystallization from the melt, α-phase is obtained. There are various process schemes to obtain β-phase. *Mechanical extension (drawing)* of α-phase is one of the most common methods where β-phase is formed. The temperature required is less than 100˚C as higher temperature does not favour its formation (most stable below 80˚C). *Copolymers* can

be *crystallized* from the melt and then grown separately on a KBr crystal. This is another way of processing the β-phase. *Electrical poling* also leads to the formation of β-phase [3].

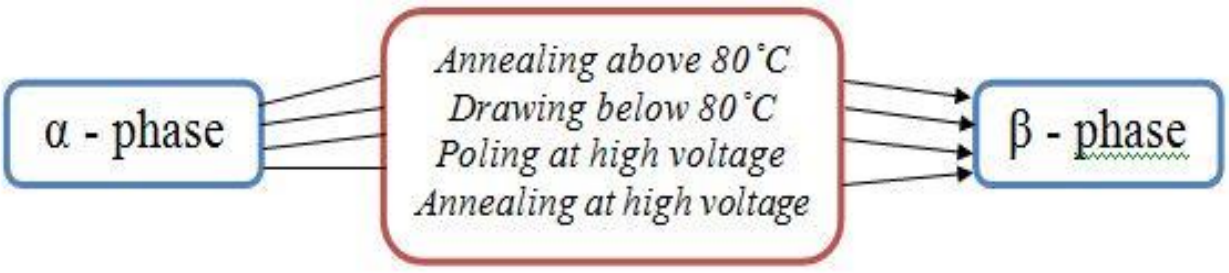

Fig. 1.4 Schematic showing formation of β-phase from α-phase [3].

When natural β- PVDF is formed it has random orientation of atoms. On application of a strong electric field, there is an alignment of dipoles which further leads to a net positive charge as seen in Fig 1.4. A high temperature (100˚C) and a strong electric field (20MV/m) are required to covert non- polar β- phase into polar one [3].

a)

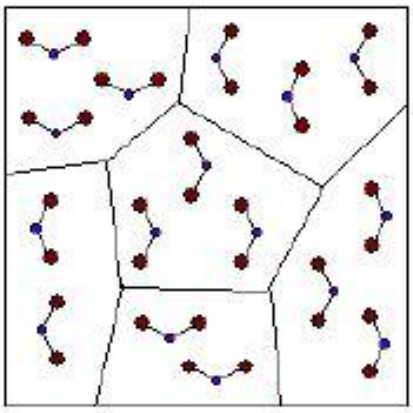

b)

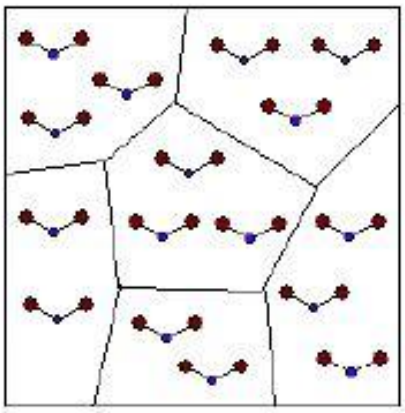

Fig 1.5a) Random orientation of dipoles in β-phase without electric field **b)** Aligned dipoles due to electric field [3].

1.6 PVDF thin films

With the advancement in technology, based on the required applications and space, thin films of PVDF can be fabricated. The fluoropolymer has an excellent chemical resistance with high dielectric strength. PVDF thin films as a two dimensional system are readily processable and possess high mechanical strength. Due to these extraordinary characteristics, thin films are being used for the manufacturing of different types of sensors. Various principles like deposition

process, characterization techniques and surfaces processes are of great importance for PVDF thin films. Moreover, β- phase films of PVDF are more stable over a long time with sequential annealing. PVDF thin films have a low acoustic impedance, comparable to water and human tissue. These films can be fabricated using numerous efficient ways such as hot- pressing, spin coating, imprinting, nano-embossing, Langmuir- Blodgett deposition etc [4, 5].

1.7 Applications of PVDF thin films

PVDF is a desirable material with potential applications in numerous fields. A good amount of work on development of thin films of PVDF is still in progress. Few of the typical applications of PVDF thin films are:

- Actuators for sound reduction and to protect certain electronic systems from noise through absorption as PVDF thin films are highly sensitive, flexible and environment resistant.
- Sensors for monitoring the structural faults in automotive, aviation and civil sectors-Reusable PVDF sensors are used which can be removed from the monitored site without damaging it.
- High sensitivity, piezoelectric behaviour and dielectric strength make it suitable to detect damages like cracks in matrix, breakage of fibres etc.
- Detection of human body by Sensor array- Due to pyroelectric nature of PVDF it is used to determine the direction of motion, presence and speed of the human body.
- In Flapping wing Micro Air Vehicles (MAVs) as Piezo actuators-Remote controlled micro aerial robots are used by defense agencies for targeting and biochemical sensing by placing high quality PVDF films on the wings.
- As pressure sensors in Aerospace engineering [8].

1.8 References

1. M.C. Rao, M.S. Shekhawat, *Int. J. Modern Physics*, 22 **(2013)** 576-582.
2. D.G. Stavenga, *Materials Today: Proceedings*, 1**(2014)** 109-121.
3. D.M. Esterly, D. Leo "Manufacturing of Poly (vinylidene fluoride) and Evaluation of its Mechanical Properties" **(2002)**.
4. J.S. Harrison, Z. Ounaies, *Encyclopedia of Poly Sci. Tech.*, 43 **(2002)**

5. T.H. Kim, A.C. Arias, *'Characterization and applications of piezoelectric polymers'*, 253 **(2015)**.
6. A. Itoh, *'Studies on the Structures and Physical Properties of Crystal Polymorphs for Poly (Vinylidene Fluoride)'*, Condensed Matter-Material Science, **(2014)**.
7. H.R. Gallantree, *Solid State and Electron Devices*, 130 **(1983)** 219-224.
8. A. Jain, A.K. Sharma, et al., *Int. J. Material Science and Engineering*, 3 **(2015)** 327-345.
9. X. Wang, F. Sun et al., *Sensors*, 18 **(2018)** 330-346.

Chapter 2

Langmuir- Blodgett Deposition Technique

Langmuir- Blodgett deposition technique is one of the methods to prepare molecular self assemblies which are imperative for fabrication of ultrathin organic films. The orientation of organic molecules at the gas- liquid interface results in the formation of a monolayer [1]. Some basic concepts and terms related to Langmuir- Blodgett technique are:

2.1 Langmuir monolayer

A monolayer or monomolecular layer formed by the crystalline arrangement of molecules at the air- liquid interface. It is a two- dimensional crystalline packing [2].

2.2 Langmuir- Blodgett monolayer

Transfer of Langmuir monolayer or multilayer onto a solid substrate produces Langmuir-Blodgett monolayer.

2.3 Gas-Liquid interface

The boundary which separates the two bulk phases- gas and liquid, marks a transition between their properties. A layer, in a metastable state, exists on the surface with completely different properties from those of the bulk [2].

2.4 Surface tension

An excess free energy is always present at the surface of the liquid because of different environments between the bulk and the surface molecules [3]. When the two phases are in equilibrium, surface tension remains constant with constant temperature. However, it is affected by the presence of a monolayer on the surface of the liquid [2]. In such experiments surface pressure is usually measured and is defined as the reduction in the surface tension of the pure liquid due to the film, i.e.,

$$\Pi = \gamma_0 - \gamma$$

where, γ_0 = surface tension of the pure liquid, i.e., in the absence of the monolayer

γ = surface tension of the film covered surface, i.e., in the presence of a monolayer [2]

2.5 LB Monolayer materials

Amphipathic or amphiphilic compounds form stable monolayers on the surface of water. The molecules of these compounds have two distinct regions: polar hydrophilic group and a sufficiently long non- polar hydrophobic group. The molecules are aligned in such a way that the hydrophilic head is immersed in the water surface and the hydrophobic tail is protruded from the water surface [4]. The simplest monolayer forming amphiphilic materials are long chain are alkanoic or fatty acids. Similarly various polymers can also be used in the same way as the long chain acids. The hydrophilic groups should be sufficient in number to allow the spreading (evenly distributed) onto the water surface and form a stable monolayer [3].

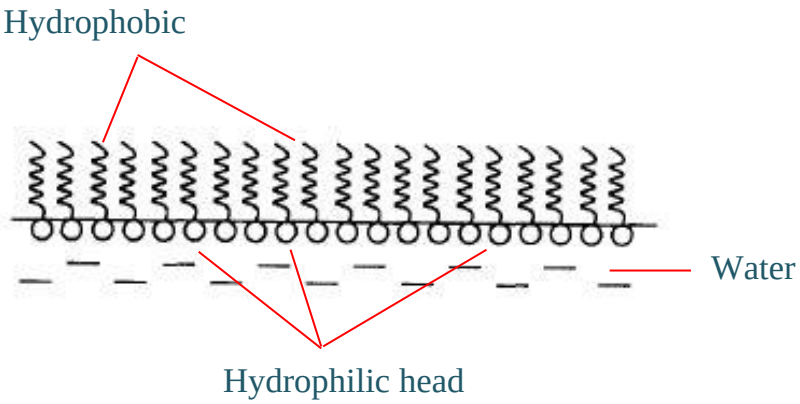

Fig 2.1 Amphiphilic molecule with distinguished hydrophobic and hydrophilic parts [2].

2.6 Surface pressure - Area isotherms

Several phase transformations occur when a monolayer is compressed on the water surface. To identify these phase changes, surface pressure (Π) as a function of area occupied by the film is monitored (Fig 2.2).. The graph so obtained is called an 'isotherm' as the measurements are carried at constant temperature. The isotherm characteristics are easy to obtain and provide useful information about the monolayers at the interface. The surface molecules do not interact when the area per molecule is high and the monolayer film is in two dimensional gas phase. Compression of monolayer leads to a rise in surface pressure indicating a change in the 2-D gas phase and a two dimensional expanded liquid state is obtained. There is an abrupt increase in the pressure and it represents a transition into a condensed phase or a solid like arrangement of molecules [1, 3].

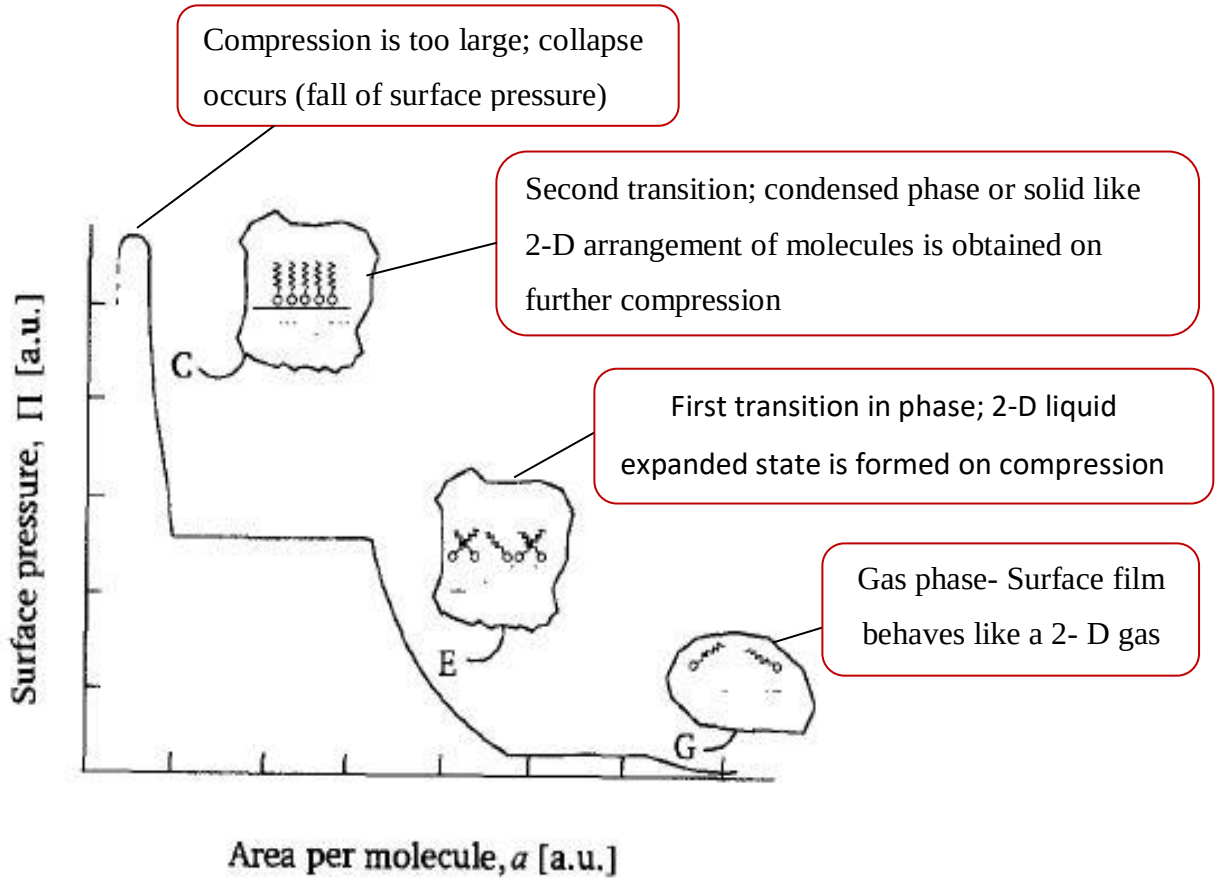

Fig. 2.2 Schematic of surface pressure- area isotherm [1, 3].

In the second phase transition when a 2-D highly ordered solid phase is formed on the monolayer, compressibility (or Young's modulus) can be calculated by the equation, (at constant temperature)

$$C = -\frac{1}{A}\frac{\partial A}{\partial \Pi} \qquad \ldots\ldots\ldots\ldots\ldots (2.1)$$

The compressibility almost reaches infinity when collapse (Π_c) occurs.

2.7 Effect of compression rate

The shape of Π- A isotherm depends on the rate of compression of the monolayer. When an insoluble monolayer at air- liquid interface is compressed, it allows us to plot a surface pressure- are isotherm. At higher compression rates, the Π-A isotherm gets shifted towards the right side. When more time is given to the solid/ condensed phase region to rearrange and homogenize, the compressibility reduces. Therefore, when monolayer is compressed at a faster rate, it results in higher compressibility (low modulus of elasticity) [8].With increase in the rate of compression, collapse pressure (Π_C) also increases [9]. All isotherms are recorded at a constant temperature.

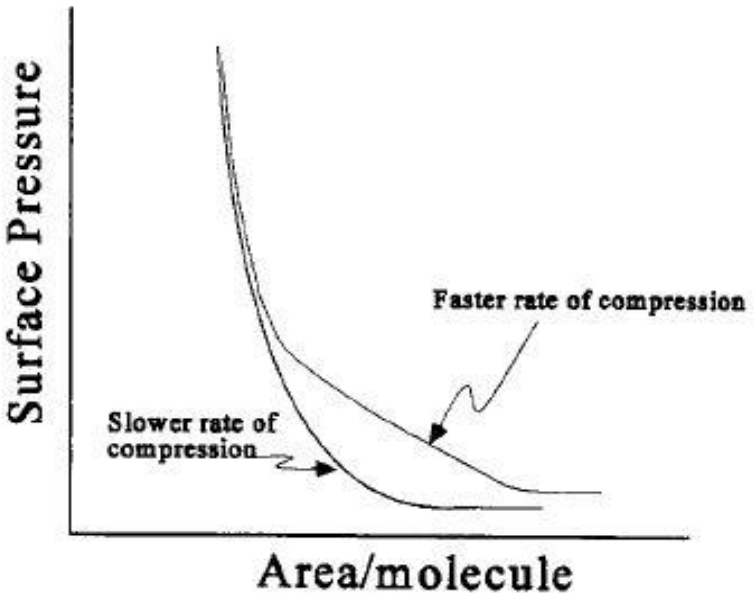

Fig. 2.3 Schematic of Π- A isotherm at different compression rates [7].

2.8 Effect of subphase temperature

With increase in subphase temperature there is a consequent decrease in the occupied area. This leads to an effective and smooth transition from gaseous to liquid phase [10]. The Π-A isotherms are recorded at different temperatures of the subphase and the compression rate is kept constant. With increase in temperature, the collapse pressure decreases. According to various studies, strain has Arrhenius temperature dependence [9].

2.9 Hysteresis

Compression and expansion cycles are obtained when the monolayer is subjected to hysteresis effect. Compression is followed by expansion by a repeated number of cycles. It is used to investigate the stability of the monolayer and exploit the phase transitions along with the molecular arrangements. Reproducibility in the hysteresis curve can be traced if the film is stable. [10]

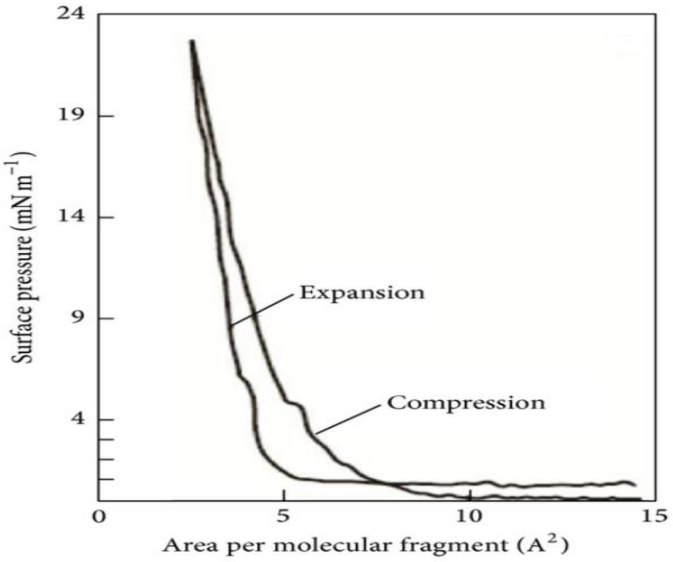

Fig. 2.4 Hysteresis curve of surface pressure- area isotherm [10].

2.10 Barrier Oscillations

The anelastic or viscoelastic properties of the monolayer are measured by the oscillations of barriers as soon as the target pressure is attained [12]. This method is useful as it allows the separation of storage (real) and dissipative (imaginary) components. The shear modulus (G*) can be calculated by the equation 2.2,

$$G^* = G' + G'' \qquad \text{..... (2.2)}$$

where G* is a complex quantity, G′ is the storage component that represents input energy during compression which gets compensated by the relaxation of stress and G″ is the dissipative component that represents input energy lost due to friction (due to viscosity) [11].

The barriers oscillate at a constant frequency of oscillation. The amplitude of the oscillations is determined by change in the area. As G′= G cosθ and G″= G sin θ

$$\text{Loss angle} = G''/G' \qquad \text{..... (2.30)}$$

For any monolayer which is highly condensed, the value of G″ is high and G′ is quite low [2].

2.11 Instrumental setup for LB technique

The Langmuir- Blodgett devices available are designed in such a way so as to effectively investigate the properties of the monolayer with precise deposition of the monolayer(s) on

desired solid substrate. Various physical descriptions and features of the LB setup are described in Fig. 2.3:

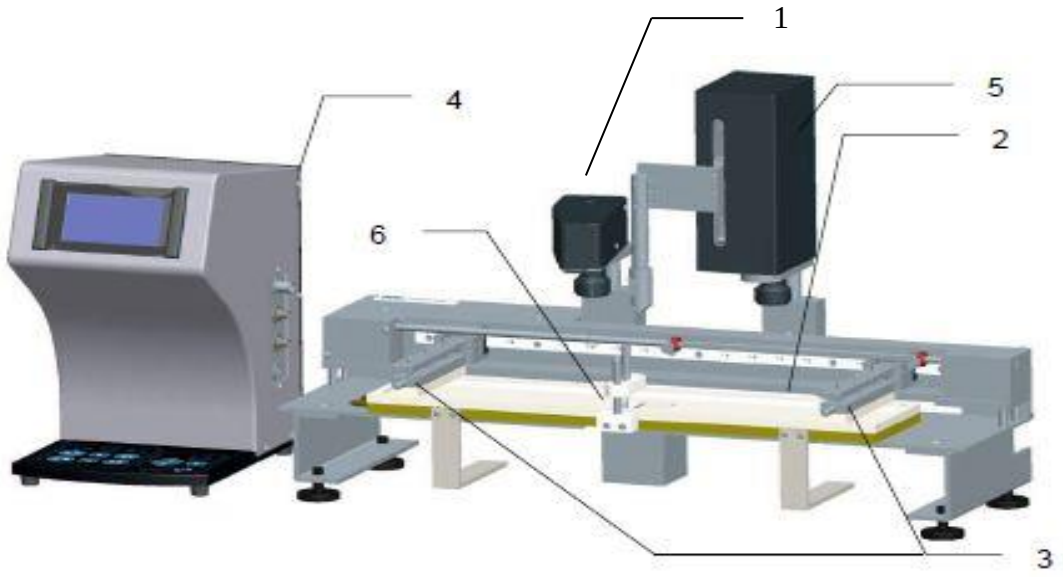

Fig 2.5 Langmuir- Blodgett setup [5]

1. Balance
2. Trough
3. Barriers
4. Layer Builder
5. Dipper
6. Well

2.11.1 Surface balance using Wilhelmy plate: The Wilhelmy plate method is used to measure the surface pressure. It is a thin plate made up of platinum (sandblasted) and is suspended on a balance. The plate is partially immersed in the subphase (water) so that a force is exerted on it which further gets converted into surface tension at the air- liquid interface (fig. 2.6).

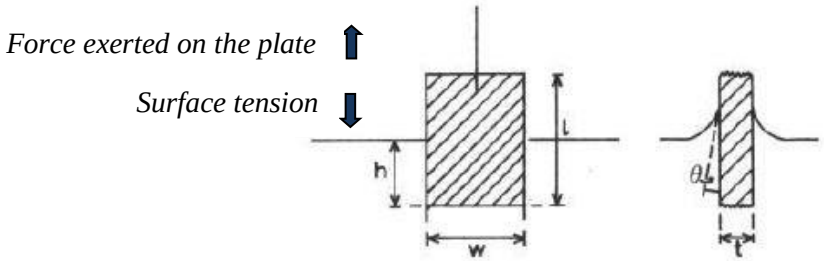

Fig 2.6 Wilhelmy plate partially immersed in subphase surface [6].

2.11.2 Trough: Langmuir- Blodgett trough top is made up of PTFE. It is hydrophobic in nature and consists of a dipping well in the centre. The trough is fixed on a plate made up of aluminium. The water bath/circulator maintains the temperature of the subphase and is connected to the trough with the special valves on both its ends [5, 7].

2.11.3 Barriers: Monolayer is compressed with the help of barriers which are made hydrophilic to ensure that the film does not escape during compression. The material used is Delrin (polyacetal). The position of barriers is controlled using the software [5, 7].

2.11.4 Layer Builder: It is an interface unit which serves as a central link between the computer and other devices connected with the LB setup. It is essential for the dipping mechanism and control of trough barriers. It provides an easy digital display [5, 7].

2.11.5 Substrate: The type of substrate used for the deposition of thin films can be either hydrophilic (glass, mica, SiO_2 etc.) or hydrophobic (HOPG etc [6].

2.11.6 Dipper Substrate attachment: After cleaning the substrate, it is attached to the arm of the dipper. It is ensured that the substrate isn't touching the inside surface of the well. Dipper is lowered slowly and the position is adjusted according to the requirement [6, 7].

2.12 Film deposition mechanism

To start the dipping process, surface pressure of the monolayer is controlled such that the film is in a stable state. Traditionally LB deposition is done when the film is in solid phase or when it is expanded so that there are enough cohesive forces between the molecules to prevent them from falling apart when transferred. The substrate is successively dipped up and down on the monolayer. Adsorption of monolayer takes place on to the solid substrate [1, 2, 6, 7].

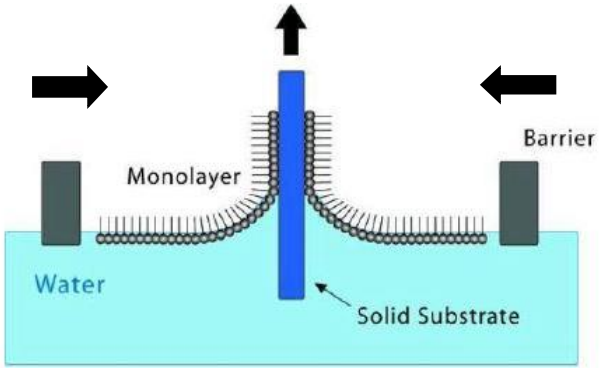

Fig 2.7 Deposition of film on a substrate [6].

2.13 Deposition modes

Nature of monolayer, substrate and subphase affects the deposition mode.

1. **X- type deposition:** This type of deposition takes place when the substrate is hydrophobic and the monolayer is transferred only during the downstroke. The monolayers are stacked in head-to-tail configuration.
2. **Y- type deposition:** In this type of mode, for hydrophobic substrate even number of layers are deposited whereas for hydrophilic substrate number of layers deposited are odd. Monolayer stacking is in a head-to-head and tail-to-tail pattern. Deposition is carried out by both upstroke and downstroke.
3. **Z- type deposition:** For the Z- type mode, the substrate should only move upwards, i.e., monolayer is deposited by upstroke only. The substrate should be hydrophilic.

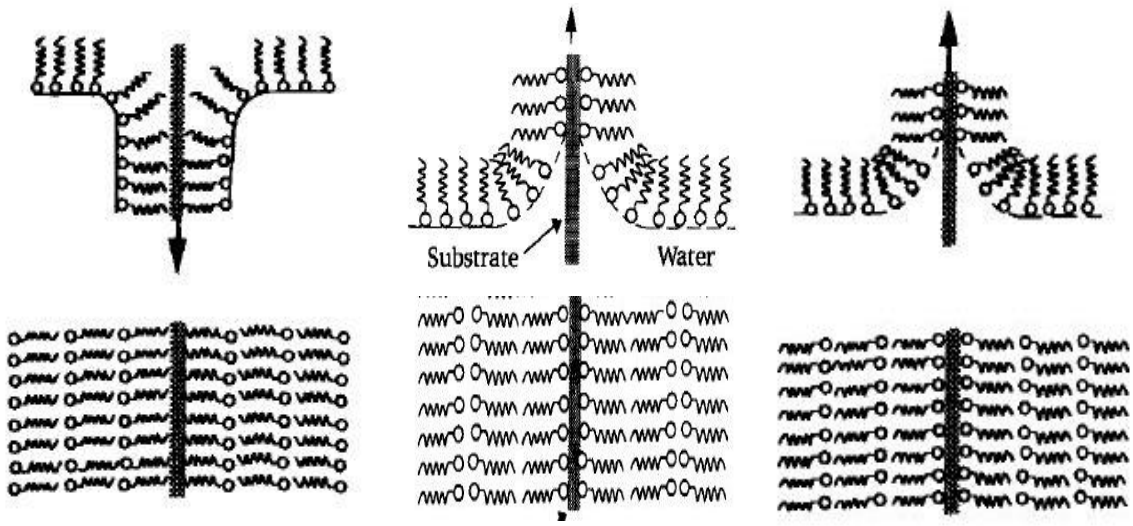

X-type Y-type Z-type

Fig. 2.8 Different modes of Langmuir- Blodgett film deposition [2].

2.14 Transfer ratio

The quality of deposition is characterized by measurement of *transfer ratio* or *deposition ratio*. It is defined as the ratio of decrease in area of monolayer removed from the water surface (surface pressure is constant) to the area of substrate coated by the monolayer. It is given by,

$$\tau = \frac{A_L}{A_S} \qquad \text{..... (2.2)}$$

Range of ideal transfer ratio is from 0.95 to 1.05. If the transfer ratio deviated from unity, it signals a change in the orientation of the molecules. For asymmetric substrates, it is not always necessary that the TR will be same for both the surfaces [2, 3].

2.15 References

1. S.A. Hussain, D. Bhattacharjee, *Modern Physics Letters*, 23 **(2009)** 1-15.
2. M. C. Petty, *Langmuir Blodgett Films* (Cambridge University Press, **1996**).
3. G.G. Roberts, *Langmuir- Blodgett Films* (Plenum Press, N.Y. **1990**).
4. O.N. Oliveria Jr., *Brazilian Journal of Physics*, 22 **(1992)** 60-68.
5. Operational Manual KSV NIMA Langmuir- Blodgett Deposition.
6. Software Manual KSV NIMA Langmuir- Blodgett Deposition.
7. Manual KSV NIMA Langmuir and Langmuir- Blodgett deposition troughs.
8. A. Jyoti, D.Y. Kwok et al., *Colloids and Surfaces*, 116 **(1996)** 173-180.
9. B. Kumar et al., *J Chem Phys*, 133 **(2010)** 70-88.
10. M. Nai, P. Lin et al., *Journal of Nanomaterials*, 10 **(2015)** 1-15.
11. K. L. Harrison, L.B. Biedermann et al., *Nanomaterials*, 31 **(2015)** 9825-9832.
12. M. Meyers, K. Chawla, *Mechanical Behaviour of Materials* (Cambridge University Press, **2009**).

Chapter 3

Literature review

Outline

This chapter deals with the compilation of various research papers which have been studied for the literature survey. The first section is relevant to the LB deposition technique for thin films and hysteresis analysis. In the second section different deposition techniques of PVDF thin films have been discussed. The remaining section pertains to LB deposition of PVDF thin films.

3.1 Deposition of Langmuir- Blodgett thin films

C. D. Bain et al 1989 [1]. Oriented organic monolayers of long chain alkanethiols were formed by adsorbance from gold solution. As gold is an inert metal, it is resistant towards contamination and does not form any stable oxide. Sulphur and gold undergo a specific interaction with the help of many functional groups present. Various characterization techniques were performed such as X- ray Photoelectron Spectroscopy (XPS), SEM, NMR spectroscopy and ellipsometry.

O. N. Oliveira Jr. 1992 [2]. Various deposition modes for LB deposition namely X- type, Y-type and Z- type was recognized. One of the most basic and fundamental characterization techniques is surface pressure- area isotherms which are dependent on parameters like subphase temperature, impurities in monolayer, compression rate and pH of subphase. The thickness of any LB film can be determined by Synchrotron X-ray reflection, X-ray diffraction, FE-SEM, etc.

M. Woolley et al 1995 [3]. Multilayer films of two cyanobiphenyl materials were deposited on number of substrates by vacuum deposition and LB technique. The films were characterized by optical microscopy, XRD. One of the material formed bilayer and the other formed a monolayer structure.

X. Chen et al 1995 [4]. Langmuir- Blodgett films of liquid crystalline polymer doped by arachidic acid (AA) were investigated by Π- A isotherms, hysteresis, X- ray diffraction and UV-Vis spectroscopy. The stability and packing of monolayer is increased by adding AA into the polymer. Phase transitions take place from liquid expanded state to solid phase at high surface pressures, subsequently forming crystallites.

J. Collins et al 2005 [5]. Langmuir monolayers of fatty acids and nematic liquid crystal were studied and transferred films were characterized by UV- Vis spectroscopy. Such films are useful in optoelectronic devices like displays. They demonstrated that other deposition techniques could not align a system which includes liquid crystals. LB technique is successful in producing such alignment.

S. A. Hussain et al 2009 [6]. Langmuir-Blodgett (LB) film deposition is used to manipulate organic materials at a molecular level for optoelectronic and electronic devices. Basic concepts of LB films were studied such as compatible material (amphiphiles), monolayer spreading and formation, deposition of Langmuir monolayer onto a substrate, etc. This technique is advantageous over other methods and is being used in fabrication of organic FETs, organic conductors and diodes, rectifiers and sensors.

3.2 Characterization of Langmuir monolayers using Langmuir troughs

S. A. Hussain et al 2009 [7]. The surface pressure is measured using the Wilhelmy plate method. It is hydrophilic in nature and is attached to an electro- balance. The solid phase is chosen for the Π- A isotherms. The dipping rate of the substrate is kept constant and at a very low value, i.e. between 1-5 mm/min.

I. N. Bhatti et al 2013 [8]. Using XRD the presence of α- and β- phases were confirmed. Due to the semi-crystalline (almost amorphous) nature of PVDF a not so sharp signature peak was observed. The thickness of PVDF thin film was evaluated using Cross-sectional SEM.

K. L. Harrison et al 2015 [9]. For graphene oxide, the viscoelasticity is measured at transfer conditions the oscillatory barrier conditions is performed. The response of area change for an ideal viscous monolayer is time dependent. There is no lag in surface pressure response to area change for an elastic monolayer whereas a phase lag of $\pi/2$ exists for a viscous monolayer. The anisotropy of surface pressure response to area change is quantified using barrier oscillation measurements by calculating the shear and elastic moduli of the monolayer.

H. Zhu et al 2015 [10]. Atomic Force Microscopy (AFM) was performed to obtain topographical features. After reaching a certain surface pressure target, PVDF (NMP)-pDDA monolayer becomes stable. The surface was smooth with a desired thickness whereas the PVDF (MEK)-pDDA monolayer was not that stable and has diamond shaped crystals.

3.3 Synthesis of PVDF thin films using various techniques

J. Sakata et al 1991 [11]. Highly oriented PVDF thin films were prepared by electrospray technique (ESP). PVDF solution was made in 0.2 wt % DMF and passed through a nozzle. A high voltage ranging between 8-15 kV was applied and then sprayed into N_2 gas. Solvent was evaporated with the help of the flowing gas and deposited on substrate. Characterization was performed by XRD and IR measurements. The pyroelectric co-efficient deduced was higher than any of the conventional PVDF films.

M. Y. Chung et al 2001 [12]. PVDF films were fabricated using vapor deposition method by applying high electric field. Temperature range for deposition was 30˚ - 90˚C and the external electric field applied was between 25 kV/cm and 1000 kV/cm. In order to fabricate high quality pyroelectric and piezoelectric films the substrate temperature is optimized. Melting point of PVDF thin films increased with substrate temperature. With the help of FTIR crystalline phases and phase transitions of PVDF were studied.

M. Benz et al 2002 [13]. Spin coating was used as a technique to fabricate thin films of PVDF due to its quickness and ability to be used on a large scale. Glass slides coated with aluminium was used a substrate. PVDF solution which consisted of 5 wt. % DMF, was spin coated and then covered with aluminium to create a capacitor. It was demonstrated that a ferroelectric material traces a butterfly- like path. Temperature was a key factor in the experiment and the samples were spun at 40˚C, 50˚C and 60˚C.

K. Pramod et al 2014 [14]. PVDF thin films were fabricated by spin coating method. The substrate was silicon wafer whose bottom layer was coated with Co by electron beam vapor technique. Using a spinner (3000, 4500 and 6000 r.p.m.) films were deposited for about one minute and then baked on hot plate at 135˚C for 10 minutes. These ferroelectric PVDF films were used in multiferroic tunnel junctions as a barrier material. The barrier width ad height can be controlled by electric and magnetic fields.

N. M. Dawson et al 2017 [15]. Direct deposition of PVDF thin films by spin coating method is studied. The films were deposited on polar and non polar surfaces where the relative humidity was ranging between 20-80%. Ferroelectric PVDF films have high dielectric constant as compared to other polymer films. PVDF was dissolved in DMSO and deposited on substrates at temperatures greater than 100˚C. Thin films were characterized by FTIR- to investigate the

crystalline phases formed, AFM and SEM - for morphology, Metal-ferroelectric-metal (MFM)- to investigate ferroelectric properties.

3.4 Synthesis of PVDF thin films by Langmuir- Blodgett deposition technique

R. C. Advincula et al 2009 [16]. Morphological and layer orientation properties were investigated by LB deposition. Various characterization techniques (spectroscopic and microscopic) such as AFM and surface plasmon resonance (SPS) were used. A phase transition was observed at 88˚C. X- ray diffraction concluded that PVDF polymer does not forms a true monolayer.

S. Chen et al 2012 [17]. LB deposition process was used to process ferroelectric β-phase PVDF ultra thin films. Dipoles were perpendicular to substrate and chains parallel to substrate. Hydrogen bonding formed between PVDF molecules and water molecules.

J. Matsui et al 2014 [18]. Properties of PVDF fluoropolymer were studied for fabrication of non-volatile memories. LB deposition was used to determine the switching characteristics and kinetics of the PVDF homoploymer. FTIR was performed and resulted in presence of 95% β-phase. Approximately no. of layers deposited on Al- coated substrate ranged between 5-35. Temperature of subphase was 20˚C. The polarization hysteresis measured the intrinsic and extrinsic switching cycles.

M. Mitsuishi et al 2015 [19]. PVDF and PVDF- pDDA films were investigated for solvent dependent properties. Two solvents were taken: N-methyl-2-pyrrolidone (NMP) and methyl ethyl ketone (MEK) and PVDF solution was prepared. Both the solvents had different interactions with the polymer. Π-A isotherms were studied and then pDDA was mixed into PVDF solution in different ratios. AFM characterized the film topography and FTIR was performed to study the hydrogen bonding in pDDA and crystal phases in PVDF-pDDA copolymer LB films.

L. Ruan et al 2018 [20]. Nanoscale PVDF thin films were fabricated using a novel and elegant self assembly method namely Langmuir- Blodgett technique. PVDF molecules are oriented on the air- water interface due to the hydrogen bonding. As PVDF thin films are highly piezoelectric and a high piezoelectric constant was acquired through this research. Amphiphilic nanosheets were used to produce oriented and smooth PVDF thin films.

3.5 References

1. C.D. Bain, J. Evall, G.M. Whitesides, *J. Am. Chem. Soc*., 111 **(1989)** 7155-7165.
2. O.N. Oliveria Jr., *Brazilian Journal of Physics*, 22 **(1992)** 60-68.
3. M. Woolley, R.H. Tredgold, P. Hodge, *Langmuir*, 11 **(1995)** 683-686.
4. X. Chen, Q.B. Xue et al., *Thin Solid Films*, 286 **(1995)** 232- 245.
5. J. Collins, D. Funfschilling, M. Dennin, *Thin Solid Films*, 496 **(2006)** 601-605.
6. S.A. Hussain, D. Bhattacharjee, *Modern Physics Letters*, 23 **(2009)** 1-15.
7. S.A. Hussain, D. Bhattacharjee, *Modern Physics Letters*, 23 **(2009)** 1-15.
8. I.N. Bhatti, M. Banerjee et al., *J. App. Phy*, 4 **(2013)** 42-47.
9. K. L. Harrison, L.B. Biedermann et al., *Nanomaterials*, 31 **(2015)** 9825-9832.
10. H. Zhu, J.Matsui et al., *Soft Matter*, 11 **(2015)** 197262- 197.
11. J. Sakata, M. Mochizuki, *Thin Solid Films*, 195 **(1991)** 175-184.
12. M.Y. Chung, D.C. Lee, *Journal of Korean Society*, 38 **(2001)** 117-122.
13. M. Benz, W.B. Euler, O.J. Gregory, *Macromolecules*, 35 **(2002)** 2682-2688.
14. K. Pramod, R. Babu, *American Institute of Physics*, 1591 **(2014)** 1039-1041.
15. N.M. Dawson, P.M. Atencio, K.J. Malloy, *Journal of Polymer Science*, 55 **(2017)** 221-227.
16. R.C. Advincula, W. Knoll et al., *J. Am. Chem. Soc*., 695 **(2009)** 192-205.
17. S. Chen, X. Li et al., *Polymers*, 53 **(2012)** 1404-1408.
18. H. Zhu, J. Matsui et al., *J. Mater. Chem. C*, 2 **(2014)** 6727-6731.
19. M. Mitsuishi, H. Zhu et al., *Soft Matter*, 11 **(2015)** 1962-1972.
20. L. Ruan, X. Yao et al., *Polymers*, 228 **(2018)** 1-27.

Chapter 4

Materials and methods

Outline

To obtain the required monolayer various materials are used. Experimental methods for the monolayer and LB film work are discussed as below.

4.1 Materials

Following are the required materials for the monolayer:

1. **Poly vinylidene fluoride (PVDF):** It is a thermoplastic fluoropolymer which serves as a monolayer forming compound on the water surface. PVDF was obtained from Alfa Aesar (= 98%). It is an apt amphiphilic material for LB thin films as the PVDF molecules on the surface of water are aligned in such a way that the C-F groups are facing down to the water (Fig. 4.1).

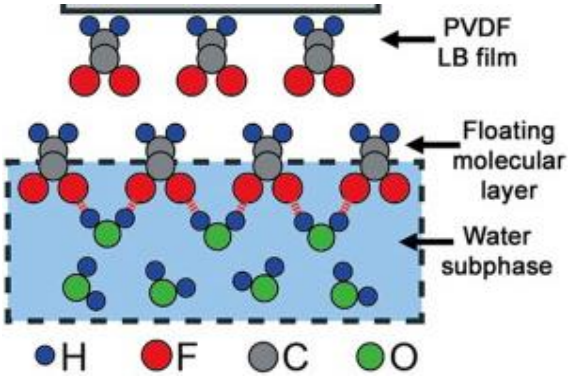

Fig. 4.1 Schematic of orientation of PVDF molecules on the surface of water**:** O-H groups forms hydrogen bonds with the C-F molecules of PVDF [5].

2. **Methyl ethyl ketone ($CH_3COCH_2CH_3$):** There are generally three types of solvent categories: *non-polar, polar protic and polar aprotic*. Protic solvents are those which have O-H or N-H bonds (which serve as proton donors) and participate in hydrogen bonding. Polar protic solvents have high dielectric constant (high polarity index). Aprotic solvents lack O-H or N-H bonds and do not form hydrogen bonds. Polar aprotic solvents have a moderately high dielectric constant (> 20) than the non polar solvents.

MEK is a *polar aprotic* solvent which is also known as Butanone (polarity index = 4.7). PVDF is dissolved in it before spreading on the subphase.

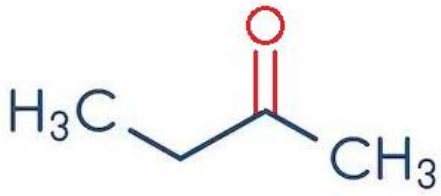

Fig. 4.2 Skeletal structure of MEK.

3. **Acetone (CH_3COCH_3):** It is an organic solvent used for the purpose of cleaning Wilhelmy plate, microsyringe, etc. It is bought from RANKEM (>99%).
4. **Methanol (CH_3OH):** It is used as a cleaning reagent for the barriers and trough. Glass slides are also cleaned with methanol after the piranha cleaning. The solvent is a product of SDFCL (HPLC grade).
5. **Propan- 2- ol ($CH_3CHOHCH_3$):** It is commonly known as Isopropyl alcohol and has a similar use in cleaning the trough and barriers. It is acquired from Fisher scientific (= 99.7%).
6. **Deionized water (Type 3):** De-ionized water is used the preparation of subphase and for cleaning purpose as well. It is obtained from Millipore Q3 deionizing system with a resistivity of 18.2 MΩcm.
7. **Glass slides:** Hydrophilic substrate used was Borosilicate glass slide. The dimensions of the slide are 26 mm x 26 mm x 1 mm.

4.2 Methods

Following experimental methods have been adopted for LB technique:

4.2.1 Cleaning the barriers and trough

Requisite cleaning of trough and barriers is essential for high quality of LB films. They are washed with methanol, propan-2-ol, distilled water and deionized water respectively.

4.2.2 Preparation of precursor PVDF solution

For monolayer spreading 0.040 mM solution of PVDF is prepared with solvent as MEK. For complete solubility, the solution is heated below its boiling point, i.e., at 70˚C in a silicon oil bath.

4.2.3 Preparation of subphase (deionised water)

DI water is used as a subphase (18.2 MΩ cm).

4.2.4 Substrate cleaning

Piranha (3:1 mixture of conc. H_2SO_4 andH_2O_2) etch solution is used to clean the borosil glass slides. These slides are then sonicated in acetone, methanol and DI water. The final glass substrate is hydrophilic.

4.2.5 Spreading of Langmuir monolayer

The subphase (DI water) is maintained at 20˚C. Using a microsyringe, 100 microlitres of PVDF solution is dispensed dropwise on the subphase surface. After 30 minutes, when the solvent gets completely evaporated. Compression on the water surface starts and pressure- area isotherms are recorded at different rates- 10, 20, 25 and 30 mm/min to a target pressure of 50 mN/m. For hysteresis, compression isotherms are recorded for 5 cycles at the 10 mm/min compression rate, keeping rest of the parameters same.

4.3 Deposition of LB monolayer on the substrate

For the film transfer process, substrate is moved through the interface of the monolayer. Speed for downstroke and upstroke are 15 and 2 mm/min respectively at Π = 20 mN/m and subphase temperature is 18˚C. The substrate is allowed to drain the water and dry for about 1 min. For the second layer deposition, the subphase is again changed and similar steps are followed for next layer deposition.

4.3.1 Drying and annealing conduct

After transferring the required no. of monolayers on the substrate, two steps are followed:

1. Substrate is kept in a vacuum desiccator and using a vacuum pump all the air and moisture is removed for about 30 minutes.
2. Annealing is conducted at about 140˚C for 4 hours, which is above the Curie temperature of PVDF.

4.4 Characterization techniques

4.4.1 Surface pressure – Area isotherms:

The isotherm characteristics very fundamental and mandatory to study the properties of monolayer(s) at the air- water interface. The Π-A isotherms have been discussed previously in

section 2.6. The typical isotherms are obtained by varying the compression rates (10, 20, 25 and 30 mm/min) and the temperature of the subphase (20, 22, 24, and 26˚C).

4.4.2 Hysteresis

Hysteresis curve is recorded for 10 cycles to analyze the stability and reproducibility of the monolayer at the air- water interface.

4.4.3 Barrier oscillations

This characterization technique is helpful in methodically examining the mechanical (visco-elastic) properties of the organized monolayer formed at the interface [3]. Oscillating barriers have been discussed earlier in section 2.10 and the measurements are made for different-

1. Oscillation frequencies (5, 10, 20, 25, 30, 35, 40, 45, 50 and 55 mHz)
2. Compression rates (10, 20, 25 and 30 mm/min)
3. Subphase temperatures (20, 22, 24 and 26˚C)

4.4.4 Atomic Force Microscopy (AFM)

Atomic Force Microscopy is categorized under high resolution scanning probe microscopy, with resolution of the order of few nanometers. The information is obtained by scanning the surface (thin film) with the help of a mechanical probe [1]. An XYZ piezoelectric sensor helps in accurate movement of the probe. There are two modes for operating the instrument- *contact mode* and *tapping mode*.

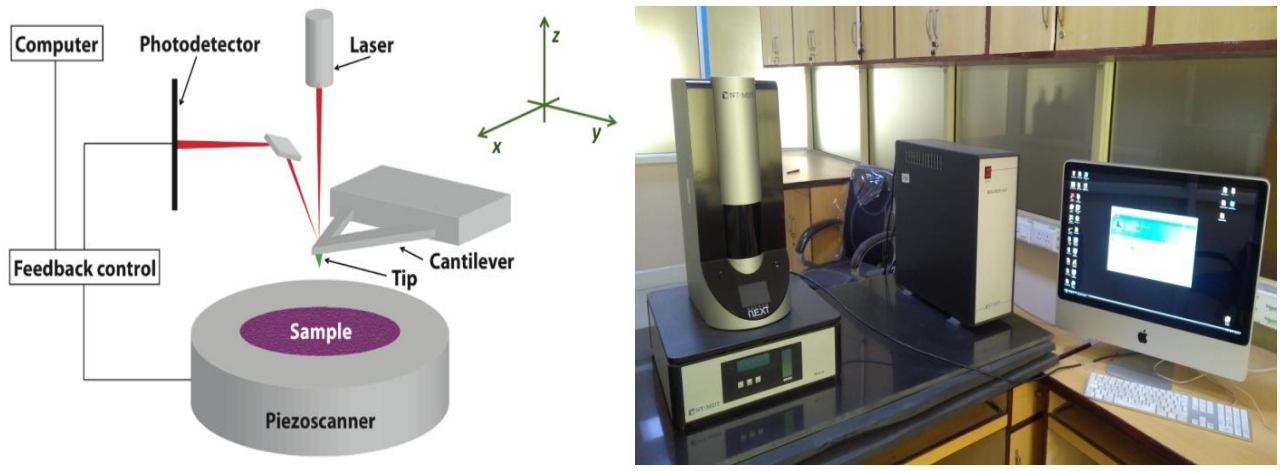

Fig. 4.3 a) Schematic diagram of Atomic Force Microscopy [1] **b)** Laboratory view of AFM used: Solver NEXT by NT-MDT.

The deflections in the cantilever (when the probe moves on the surface) are measured by the detector and the interatomic interactions are observed on the computer [4]. AFM is used to determine the shape and size of grain and along with the surface roughness.

The AFM is performed for various PVDF thin films samples prepared with varied number of layers (1, 4, 8 layers) in non-contact mode on NT-MDT Solver Next. The topographical view of the surface of PVDF thin film is obtained and roughness value is measured.

4.5 References

1. S. Chakraborty, *'Investigations of molecular organization in organo-clay multilayer hybrid films fabricated by LB and Layer-by-Layer self assembly technique'*, PhD Thesis, Tripura University, **(2015)**.
2. Julio A. N. Soares, *Practical Materials Characterization* (Springer Science, **2014**).
3. K. L. Harrison, L.B. Biedermann et al., *Nanomaterials*, 31 **(2015)** 9825-9832.
4. J. A. Zasadzinski, M. L. Longo et al., *Colloids and Surfaces A: Physiochemical and Eng. Aspects*, 93 **(1994)** 305-333.
5. S. Chen, K. Zeng et al., *Polymers*, 53 **(2012)** 1404-1408.
6. K. Inaba, T. Endo et al., *Advances in Material Phy. And Chem*., 3 **(2013)** 72-89.
7. I. N. Bhatti, M. Banerjee et al., *J. App. Phy*., 4 **(2013)** 42-47.

Chapter 5

Results and discussion

Outline

In this chapter experimental results obtained from various characterization techniques like surface pressure-area isotherms, hysteresis experiments, Oscillating barrier experiments, dipping and AFM have been discussed.

5.1 Surface pressure- Area (Π-A) isotherms

Π-A isotherms for Langmuir monolayers are the most basic characterization tool. They provide information regarding molecular level phenomenon and are also useful in estimating the monolayer stability. The instantaneous deformation in the Langmuir monolayer can be directly measured in the absence of any dissipative effects. Hence, the slope of isotherm gives the value of *Static elasticity*.

$$E = -A\frac{d\Pi}{dA} \quad \text{..... (5.1)}$$

Units of elasticity or compressing modulus, E are ***mN/m***.

5.1.1 Effect of compression rate

The Π-A isotherms for PVDF homoploymer at different compression rates are shown in fig. 5.1(a). Table 5.1 depicts mean molecular area (MMA) for liquid and solid phases as well as the static elasticity of the solid phase for all the isotherms. Compression rate directly influences the MMA of liquid and solid phase as well as the static elastic constant of the solid phase (figure 5.1(b)).

Table 5.1 Mean molecular area (MMA) of liquid and solid phases and static elasticity of the solid phase for different compression rates.

Rate (mm/min)	MMA of liquid phase (Å²/molecule)	MMA of solid phase(Å²/molecule)	Elasticity (mN/m)
10	0.505	0.411	87.58
20	0.630	0.525	64.97
25	0.632	0.527	71.017
30	0.739	0.637	63.666

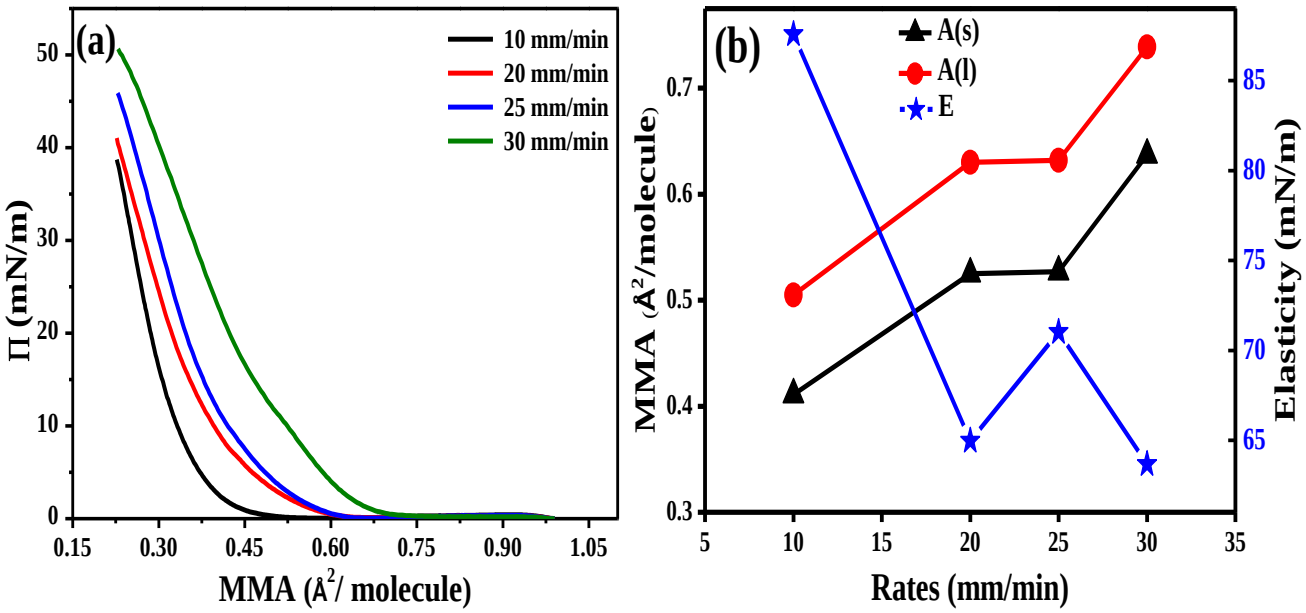

Fig. 5.1 ***Effect of compression rate*** **a)** Π- A isotherms for PVDF at 20˚C on DI water for spreading volume of 100 μL **b)** Variation of MMA of solid and liquid phase and static elasticity of solid phase with different compression rates.

Various studies with certain supporting techniques such as BAM have concluded that increase in rate of compression shifts the lower part of isotherm towards the right side. At lower compression rates, more amount of time is provided to the 2D condensed phase molecules to rearrange themselves and tightly bound together. Thus, this leads to decrease in compressibility or increase in the static elasticity [1, 2]. This is also seen in the present system with the monolayers formed for 10mm/min have the highest elasticity and lowest MMAs. The collapse pressure also increases for higher compression speeds. Polymeric monolayers are more rigid than simple amphiphiles [3].The results of Fig. 5.1 allows us to choose the adequate compression rate of 10 mm/min as it is low enough to permit stable solid phase to coalesce, which in turn reduces the compressibility**.**

5.1.2 Effect of subphase temperature

Fig 5.2 (a) shows the Π-A isotherms for PVDF with subphase temperature variation. It is clearly visible from fig. 5.2 (a) that the collapse pressure decreases with increase in the subphase temperature. The compression of monolayer shows Arrhenius temperature dependence [2].

Table 5.2 and fig. 5.2 (b) provides an overview of MMA of liquid and solid phases in addition to the static elasticity of PVDF monolayer at various subphase temperatures. High polymeric chain rigidity can be observes at lower temperatures [3].

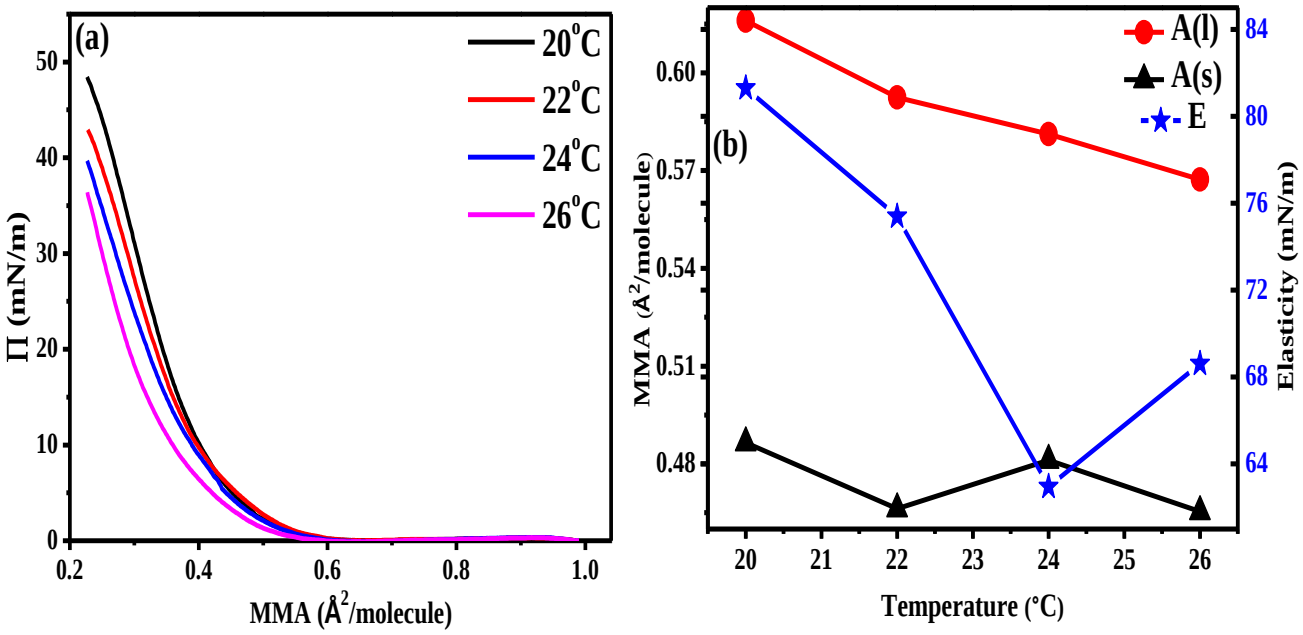

Fig. 5.2 ***Effect of subphase temperature*** **a)** Π-A isotherms for PVDF at 10 mm/min barrier speed for a spreading volume of 100µL **b)** Variation of MMA of solid and liquid phases and static elasticity of solid phase with different subphase temperatures.

Table 5.2 MMA of liquid and solid phases and static elasticity for different subphase temperatures.

Temperature (˚C)	MMA of liquid phase (Å²/molecule)	MMA of solid phase (Å²/molecule)	Elasticity (mN/m)
20	0.616	0.4865	81.293
22	0.5925	0.4662	75.39
24	0.5812	0.4811	62.954
26	0.5673	0.4654	68.612

It can be deduced from fig. 5.2 (b) that there is no drastic effect on the MMA of solid phase when the subphase temperature is increased from 20 – 26 °C. But we see a very large decrease in elasticity. This can be understood in terms of the motion of the molecules on the subphase

surface. The kinetic energy of the molecules increases with temperature which is decreasing the stability of the film inspite of no large change in MMA.

5.1.3 Hysteresis

Hysteresis Π-A isotherms provide information regarding the conformational behaviour of PVDF under the influence of compression and expansion cycles. In order to study the molecular packing and intermolecular forces between the two dimensional structured phases hysteresis experiment is performed. The compression-expansion isotherms are shown in fig. 5.3 for 5 cycles at optimized conditions: compression- expansion speed of 10 mm/min, subphase temperature as 20˚C and attaining a maximum pressure of 35mN/m.

The stability and nature of monolayer is also dependent on the spreading solvent used. MEK can is a good swelling agent and can swell PVDF during the dissolution process [4]. The diffusion rate of the solvent into the polymer is much higher. Therefore, due to compression PVDF compacts steadily to form stable monolayer at the air-water interface and the degree of molecular interactions increases. The second cycle does not retrace the first one; however the successive cycles almost coincide [5]. This indicates that the state of monolayer remains preserved during the subsequent compression and expansion cycles (fig 5.3 (a)).

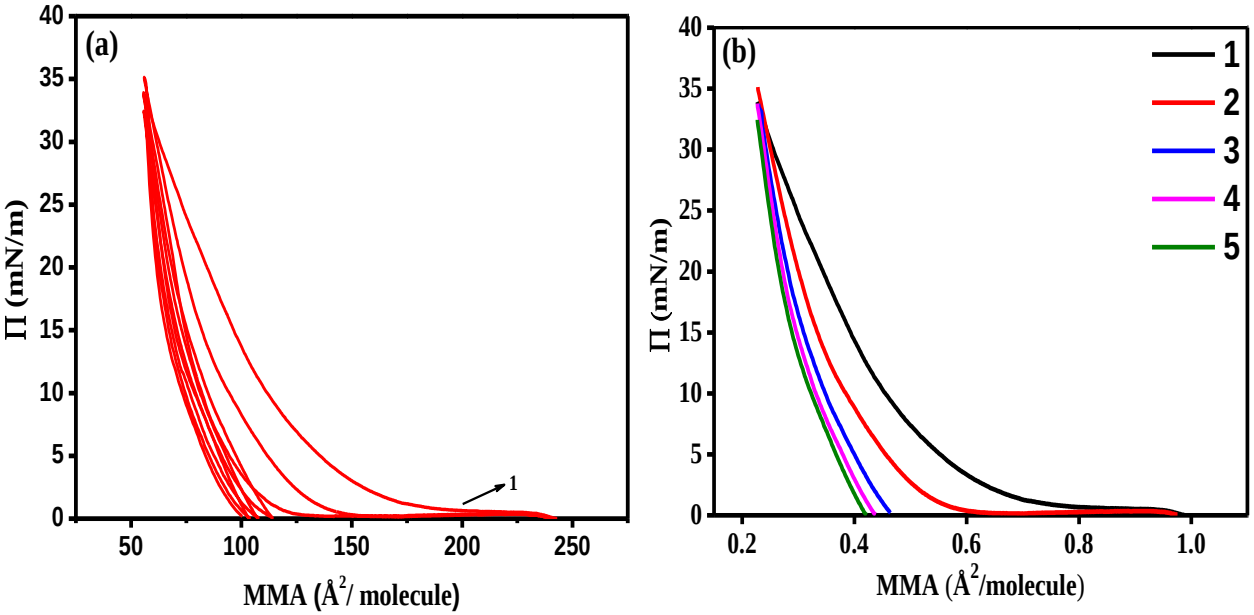

Fig. 5.3 a) Π-A hysteresis isotherms of PVDF monolayer for 5 cycles **b)** Compression isotherms hysteresis at rate 10 mm/min with spreading volume 100µL and subphase temperature 20˚C.

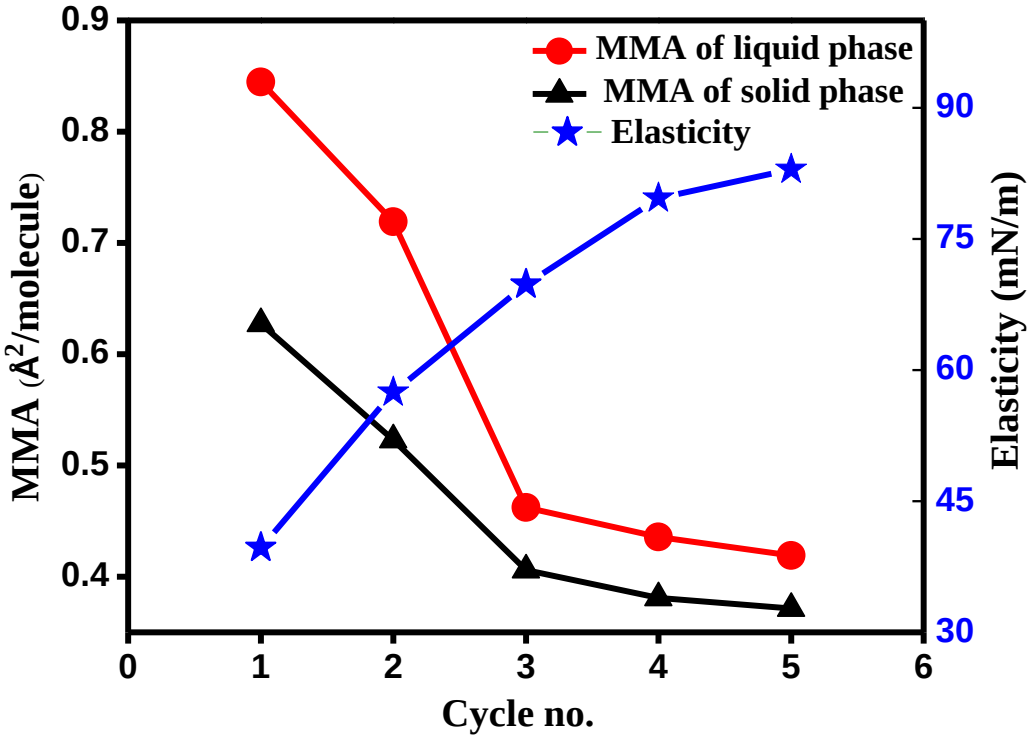

Fig. 5.4 Variation of MMA of liquid and solid phase and static elasticity with the number of cycles.

Table 5.3 MMA and static elasticity of liquid and solid phases for successive compression cycles during hysteresis study.

No. of Cycles	MMA of liquid phase (Å²/molecule)	MMA of solid phase (Å²/molecule)	Elasticity (mN/m)
1	0.8446	0.6273	39.71
2	0.7189	0.523	57.451
3	0.4623	0.406	69.802
4	0.4357	0.3809	79.664
5	0.4189	0.3713	82.951

It is observed from fig. 5.4 that there is a steady decrease in the MMA of both liquid and solid phases as and when the monolayer is subjected to compression. The elastic constant of solid phase increases when the monolayer becomes more compact. Upon lateral compression the area of monolayer decreases while the number of surfactant molecules remains same. Some amount of hysteresis can be seen during the first three compression cycles as compared to the remaining two where it is less.

5.2 Oscillating barrier characterization of PVDF Langmuir monolayers

The characterization technique of barrier oscillations is used to deduce the dynamic elasticity (viscoelasticity) of monolayer(s). The measurements of dynamic elasticity provides information regarding the forces of interaction within the thin film therefore, for PVDF monolayer the measurements were performed in the condensed phase at a surface pressure target of 30 mN/m and 10 mm/min barrier speed. The dynamic anelastic properties namely, G (Elastic modulus), G' (Storage modulus) and G" (dissipative or viscous modulus) are determined using an inbuilt software of the Langmuir Blodgett trough system for various oscillation frequencies.

5.2.1 Effect of barrier oscillation frequency

The concept of relaxation process is involved in the measurement of dynamic elasticity. So, the time scales play an important part here. Firstly barrier oscillations were recorded at different frequencies ranging between 5 to 55 mHz (in steps of 5 mHz). One necessary condition for the frequency of oscillation is that the sinusoidal wave generated cannot be slower than the barrier speed and if it is too fast, the relaxation processes do not become recognizable. The frequencies are decided according to the literature review of similar systems [4]. For this characterization technique the barrier speed was 10 mm/min and subphase temperature as 20˚C with the same spreading volume. The monolayer is compressed to a target of 35 mN/m. Thereafter the barriers start to oscillate. Fig 5.5 shows $\Delta\Pi$ variations with time during the measurement of dilational properties. The data obtained for the interfacial/ viscoelastic properties is depicted in table 5.4 and fig 5.5.

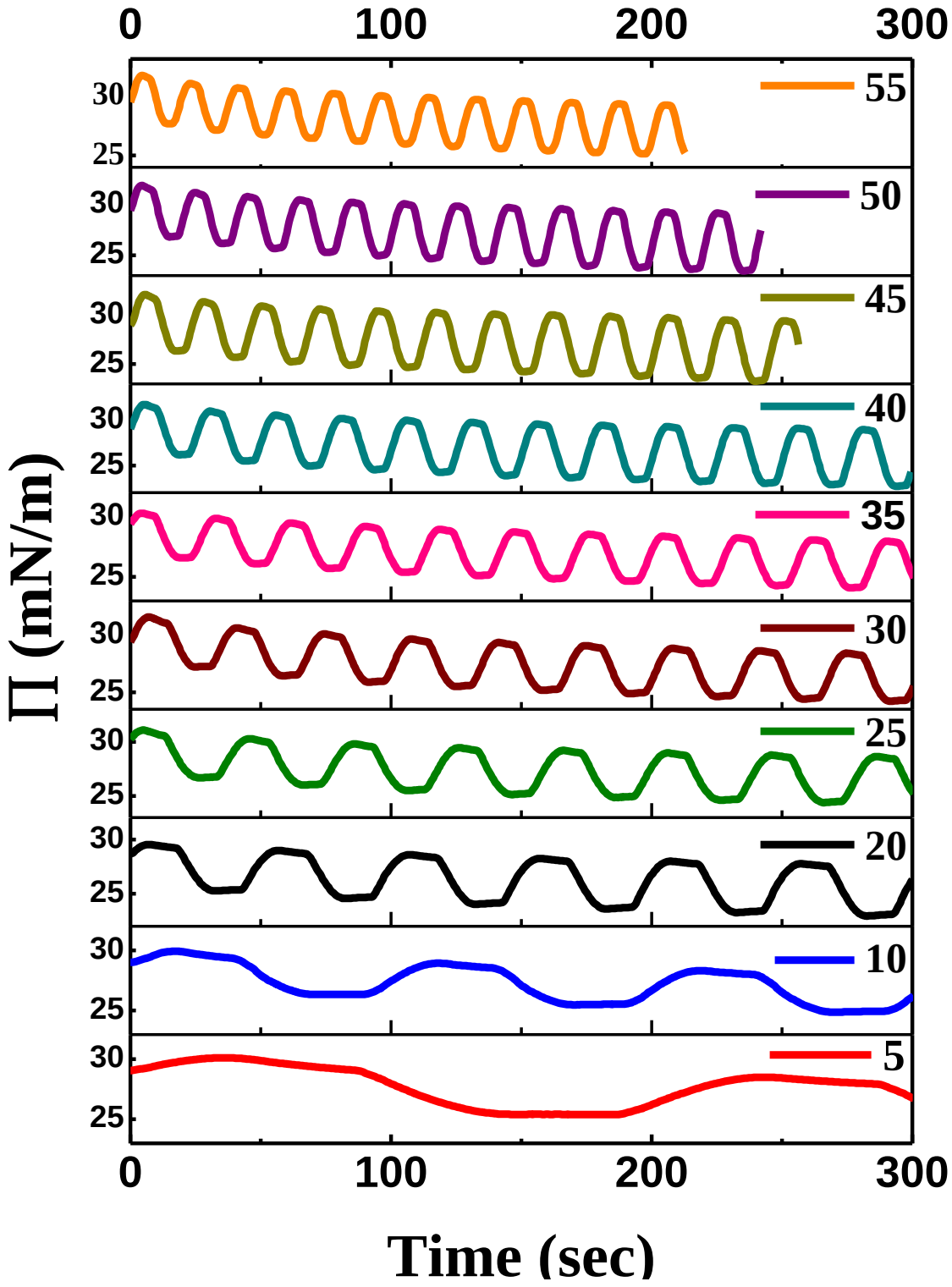

Fig 5.5 Surface pressure variations with time at different oscillation frequencies for PVDF monolayer with barrier speed 10 mm/min.

Table 5.4 Dynamic viscoelastic properties at different oscillation frequencies.

Frequency (mHz)	|G| (mN/m)	G' (mN/m)	G" (mN/m)
5	211.54	151.69	147.44
10	486.23	318.36	367.51
20	69.54	62.36	30.78
25	53.23	53.2	1.64
30	234.57	140.61	187.75
35	79.21	34.83	71.14
40	939.55	131.97	930.23
45	82.24	75.47	32.68
50	184.46	68.1	171.43
55	73.97	71.46	19.09

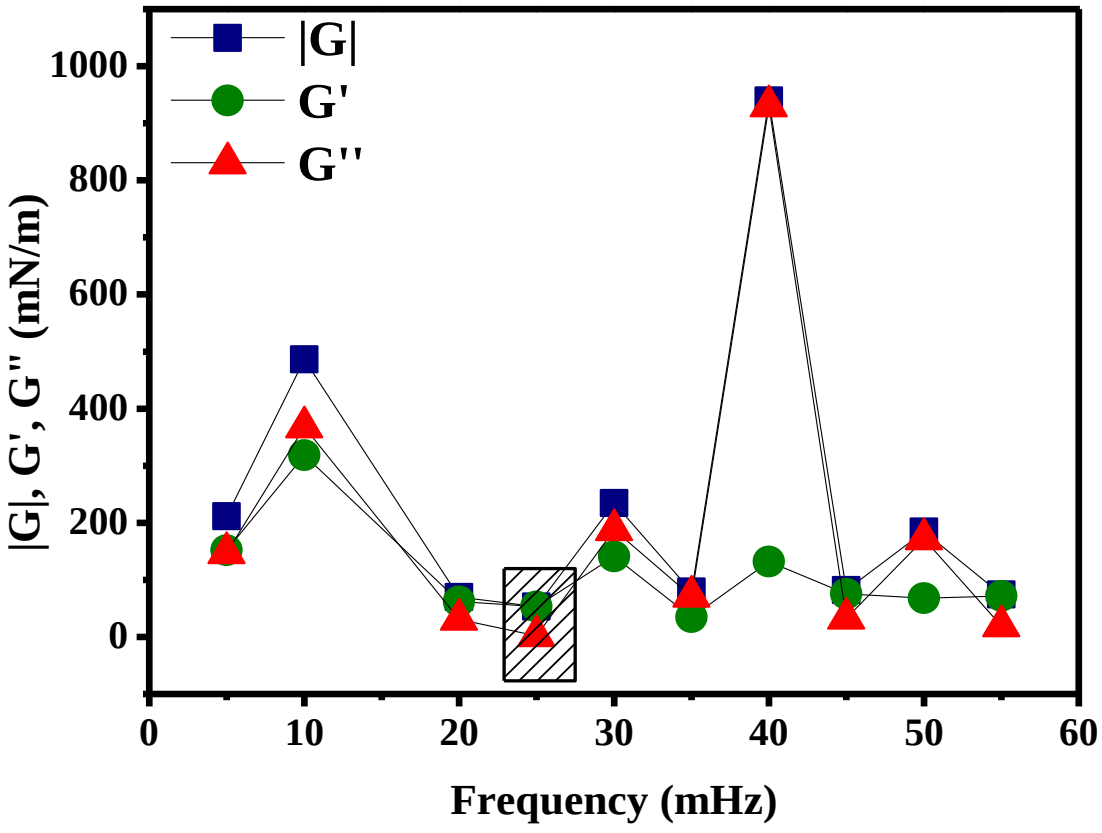

Fig. 5.6 Variation of |G|, G', G" with different barrier oscillations frequencies.

From the fig 5.6 one can deduce that at 25 mHz the dissipative modulus is the least and the storage modulus is same as the dynamic elasticity of PVDF monolayer. At 40 mHz dissipative loss is the highest. The stability of the system is known to be at 25 mHz. Therefore, the effect of compression rate and subphase temperature is observed at an oscillation frequency which is fixed at 25 mHz.

5.2.2 Oscillation of Barriers at different compression rates

The compression rate is useful in determining the elastic properties of PVDF monolayer which can be traced by the Π-A isotherms.

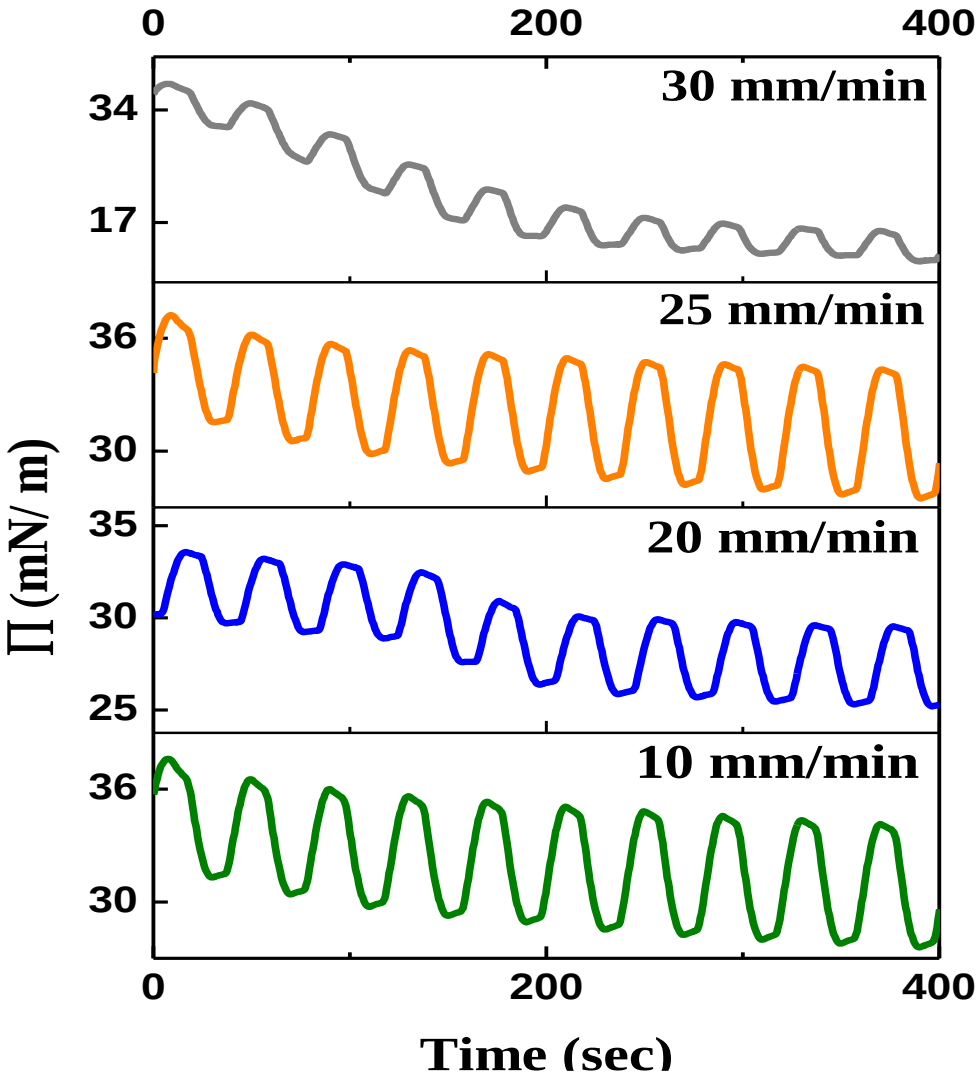

Fig 5.7 *Π-A* variations for barrier oscillation experiments for different compression rates at barrier oscillation frequency 25 mHz and subphase temperature 20˚C.

To understand the effect of rate of compression on the elastic and viscoelastic/anelastic properties of the monolayers oscillating barrier experiments were performed for different compression rates: 10, 20, 25 and 30 mm/min. Fig 5.7 demonstrates surface pressure oscillations for various rates of compression whereas Table 5.5 & Fig 5.8 signify variation in dynamic viscoelastic properties obtained from the analysis of curves.

Table 5.5 Dynamic viscoelastic properties obtained from the analysis of the curves at different rates of compression.

Rate (mm/min)	|G| (mN/m)	G' (mN/m)	G" (mN/m)
10	92.77	91.93	12.51
20	55.7	49.44	25.65
25	93.32	90.4	23.16
30	108.51	81.22	71.96

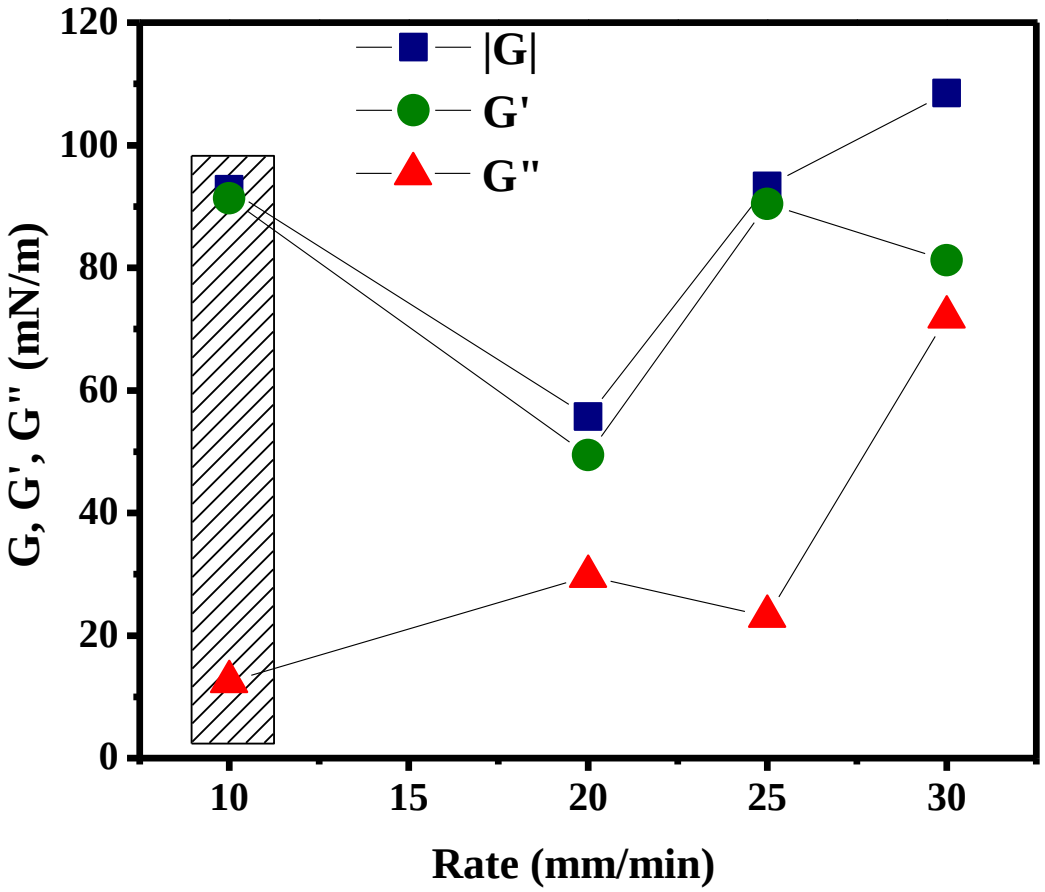

Fig. 5.8 Variation of |G|, G' and G" at different compression rates for PVDF monolayer.

From the analysis of the data obtained it is found that the compression rate of 10 mm/min is appropriate as the dissipative modulus (G") is the least and the storage modulus (G') is approximately equal to the elastic modulus (G).

5.2.3 Oscillation of barriers at different subphase temperature

Elastic and dynamic viscoelastic properties are deduced using the oscillating barrier method performed for different temperatures: 20, 22, 24 and 26˚C. Fig 5.9 shows the variations in surface pressure with time for different subphase temperatures. The data recorded in table 5.6 and Fig. 5.10 depicts the change in dynamic anelastic properties which are obtained by the analysis of curves.

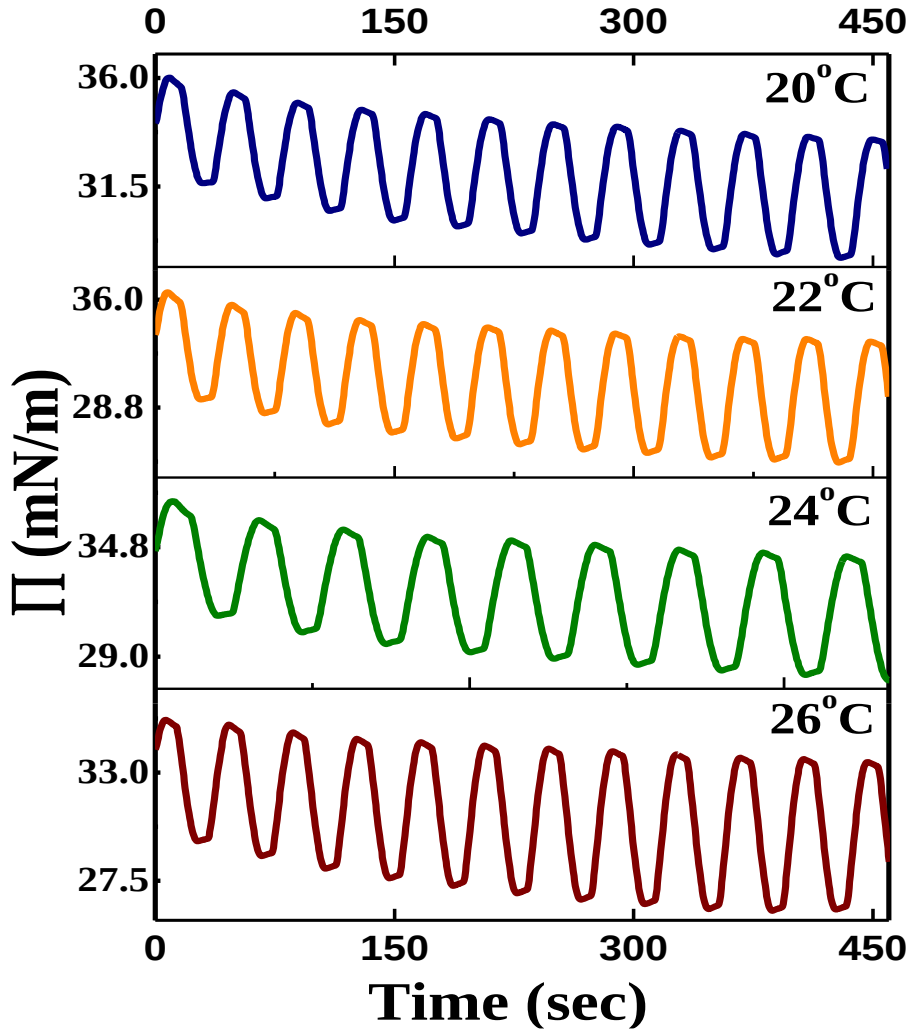

Fig 5.9 Surface pressure variations for barrier oscillation experiments at different subphase temperatures with barrier speed 10 mm/min and frequency of oscillation as 25 mHz.

Table 5.6 Dynamic viscoelastic properties obtained from the analysis of curves at different subphase temperatures.

Temperature (˚C)	|G| (mN/m)	G' (mN/m)	G" (mN/m)
20	356.07	297.74	195.29
22	375.26	28.07	374.21
24	89.73	87.75	18.75
26	50.87	50.87	17.95

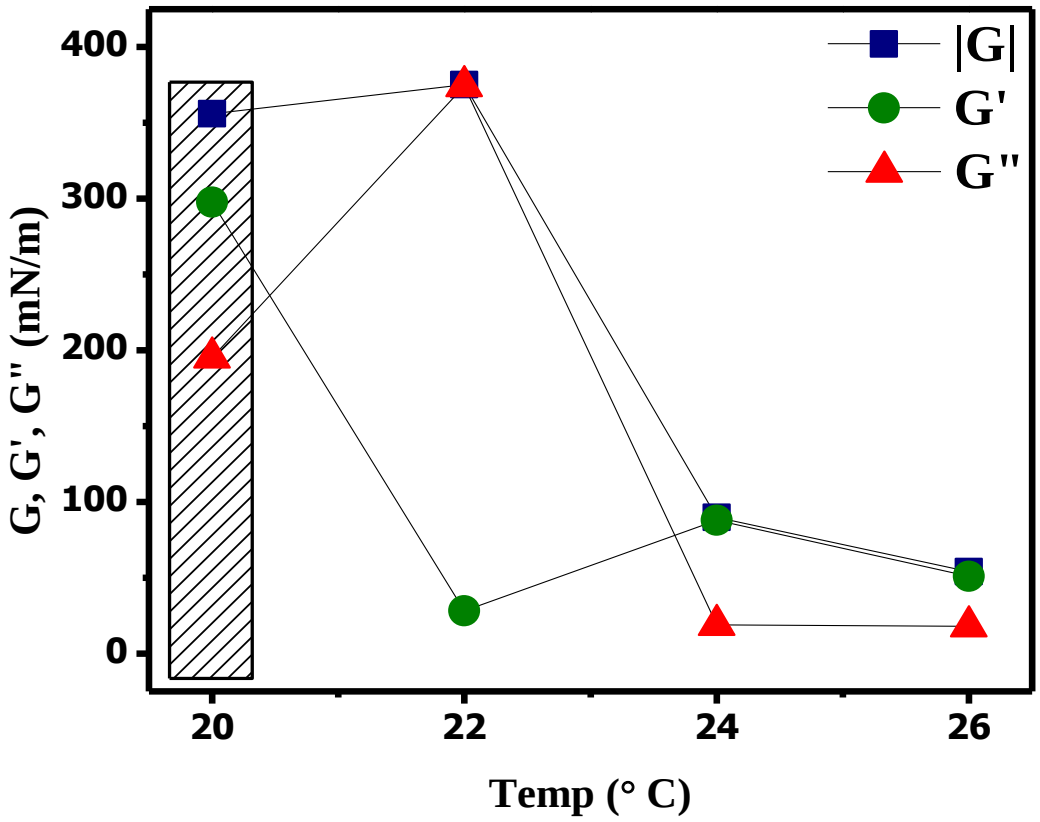

Fig 5.10 Variation of G, G' and G" with subphase temperature at a compression rate 10 mm/min.

It was concluded from fig. 5.10 that a 22˚C subphase temperature results in a large dissipative event for elastic modulus. At 24˚C and 26˚C the loss and storage modulus are almost constant. When the subphase temperature is 20˚C high value of storage modulus and elastic modulus compensates for the dissipative modulus.

Final dipping parameters: A complete characterization of the as synthesized PVDF Langmuir monolayers using static Π-A isotherms, hysteresis as well as the dynamic oscillating barrier techniques allows for us to determine the trough parameters for the most stable PVDF monolayer:

Compression rate: 10 mm/min

Temperature: 20˚C

Also all the depositions were started with the hydrophilic glass substrate already dipped in the subphase before the spreading of the PVDF monolayer. So, first movement of the dipper is always upstroke.

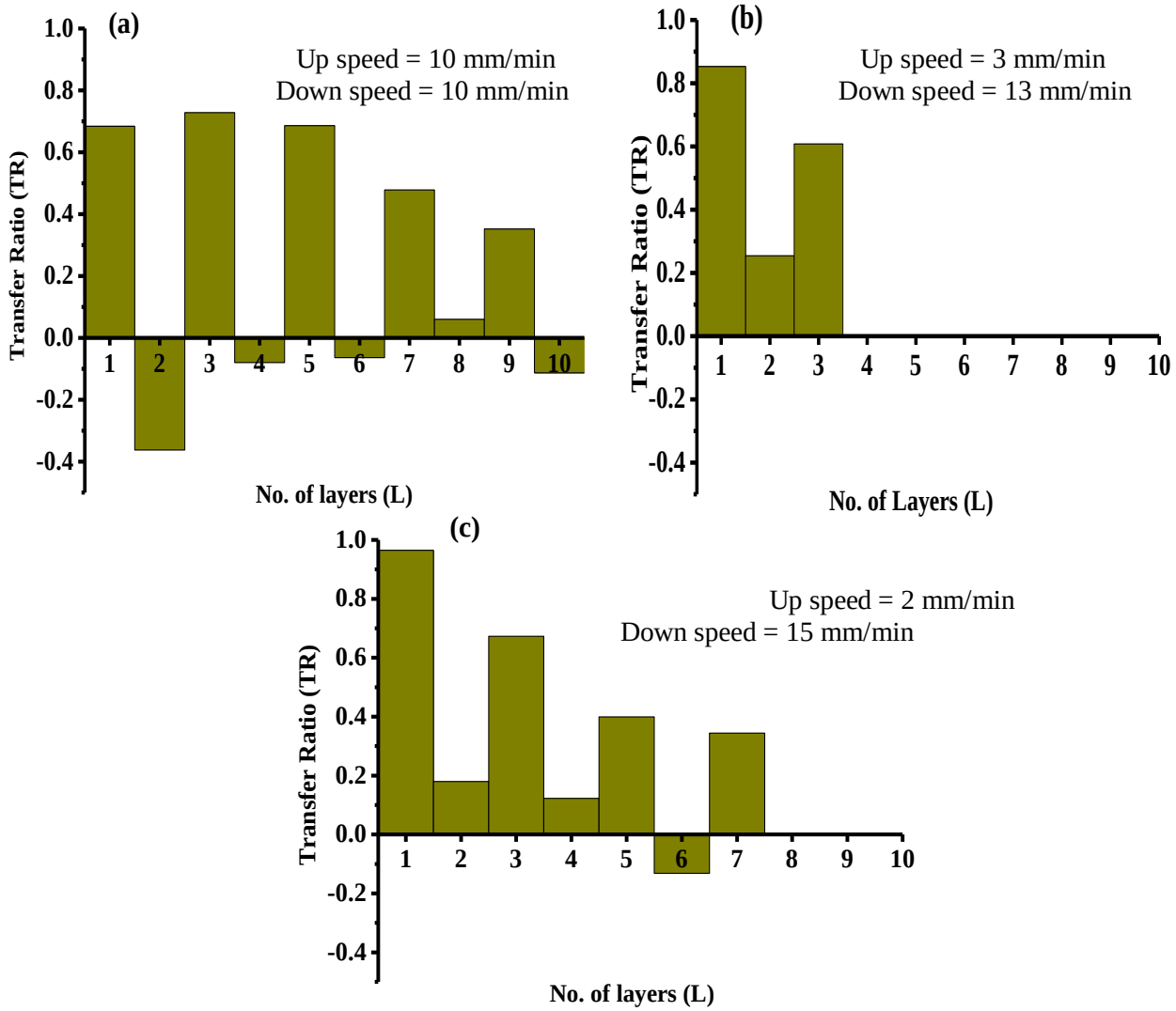

Fig 5.11(a-c) Variation of Transfer ratio (TR) with No. of layers of PVDF monolayer at different dipping parameters with surface pressure target 30 mN/m.

5.3 Deposition of PVDF Langmuir Blodgett films

Target surface pressure was determined from the location of the elasticity maxima in the solid phase and set to 30mm/min. The final parameter which needs to be set is the rates: the upstroke and the downstroke rates. Transfer Ratios (TR) for the Langmuir –Blodgett transferred onto the hydrophilic substrate (glass) under various conditions is shown in Fig 5.11.

For high values of upstroke and downstroke speeds, i.e., 10 mm/min the TR is unsatisfactory. First layer gets partially deposited on to the substrate with a TR of 0.7. However, the TR of more than one layer was not sufficient. For every downstroke of the dipper, the PVDF molecules get desorbed resulting in a negative transfer ratio (fig. 5.11(a)). The film transfer is made only during the upstroke. When the dipping speed is altered to 3 mm/min for up and 15 mm/min for down stroke the transfer Ratio for the first film improves (fig. 5.11(b)). For effective transfer of PVDF monolayer, last condition is selected where the dipping speed for upstroke and downstroke is 2 mm/min and 15 mm/min respectively (fig. 5.11(c)). This yields a good TR which is almost unity.

It was observed that though the films are getting transferred on all the upstrokes the TR reduces drastically after the first stroke. Also either the film desorbs or does not get adsorbed during the downstroke. So only one layer was deposited at a time i.e. after the first layer has been deposited the surface pressure was released and the trough was cleaned to prepare for the next monolayer. For the second and subsequent layers the substrate was hung just above the surface of the water to avoid the dissolution of the already deposited film.

In this manner 1, 4, and 8 layers were transferred. And the same were annealed for the final phase formation.

5.4 Atomic Force Microscopy (AFM)

The PVDF LB films formed with transfer of 1, 4, and 8 layers were characterized topographically after the β-phase formation using AFM.

The analysis of the AFM images (fig 5.12, table 5.7) of the films clearly shows that the films are rough in nature and become more so progressively as the number of layers increases. The scan of the area between the large crystallites for 1 layer sample (fig 5.12(b)) shows that this area is very smooth with r.m.s roughness of ~ 6 nm.

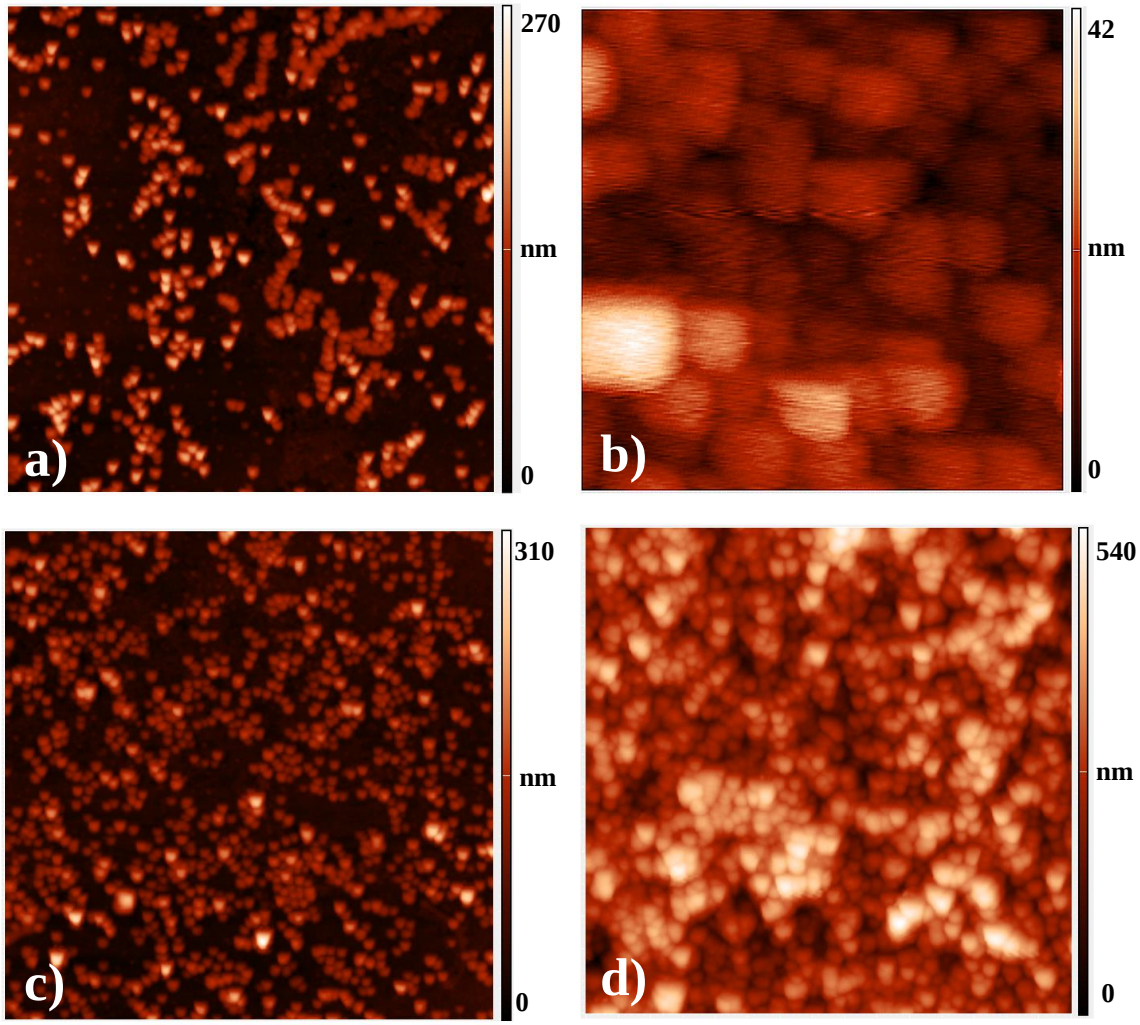

Fig 5.12: AFM images of PVDF Langmuir-Blodgett films on glass substrate a) 20 μm ×20 μm image of 1 layer b) 1 μm ×1 μm, image of 1 layer film in the smoother region c) 20 μm ×20 image of 4 layer film, d) 15 μm ×15 μm image of 8 layer film.

Table 5.7: Roughness analysis of the AFM images

Layers Transferred	r.m.s. Roughness (nm)
1	44.7
4	44.2
8	80

5.5 References

1. A. Jyoti, R.M. Prokop et al., *Colloids and Surfaces,* 116 **(1996)** 173-180.
2. B. Kumar, K.A. Suresh et al., *J. Chem Phys*., 133 **(2010)** 1836-1849.
3. C.P.L. Rubinger, R.L. Moreira et al., *App. Surface Sci*., 253 **(2006)** 543-548.
4. W. Ma, J. Zhang et al., *Journal of Macromolecular Science,* 47 **(2008)** 434-449.
5. T. Reda, H. Hermel, H.D. Holtje, *Langmuir,* 12 **(1996)** 6542-6458.

Chapter 6
Conclusion and future scope

6.1 Conclusion

Methyl ethyl ketone (MEK, polar aprotic) was used as solvent for PVDF. To obtain good transfer characteristics the PVDF monolayers on the water surface were characterized for different compression rates and subphase temperature. The isotherm, hysteresis and barrier oscillation experiments show that the most stable PVDF films were obtained at 20 ˚C for 10 mm/min compression rate. These trough parameters were used for the deposition of the LB films. An important result to emerge from these experiments was that even though the MMA of the solid phase does not change significantly with the temperature range under consideration the enhanced kinetic energy drastically reduces the elasticity of the solid phase at higher temperatures. The dipping experiments show that very good TR can be obtained for the first upstroke for 2 mm/min substrate speed. But down stroke results in partial desorption and reduced TR in subsequent upstrokes. This indicates that PVDF LB films are Z-Type in nature. But the Z-Type nature gets disrupted due to the partial dissolution of PVDF into water during downstrokes. To avoid this the subphase was changed after every single layer deposition. Transparent films of PVDF were synthesized by deposition of 1, 4 and 8 layers on the hydrophilic substrate followed by drying and annealing. The topographic analysis of the final films shows the emergence of few large crystallites which makes the films rough.

6.2 Future scope

The LB deposited PVDF films should be studied further to understand the effect of annealing temperature and time on the topography of the final films.